# Supporting information

# Synthesis and Structure of New Methylene-bridged hexopyranosyl nucleoside (BHNA)

Chuanzheng Zhou, Oleksandr Plashkevych, Yi Liu, Naresh Badgujar, Jyoti Chattopadhyaya*

Department of Bioorganic Chemistry, ICM, Box 581, Biomedical Center, Uppsala University, SE-751 23 Uppsala, Sweden

jyoti@boc.uu.se

Table of Content:

**General Experimental Methods Section.**

Chromatographic separations were performed on Merck G60 silica gel. Thin layer chromatography (TLC) was performed on Merck pre-coated silica gel 60 F254 glass-backed plates. $^{1}H$ NMR spectra were recorded at 600 MHz and 500 MHz NMR, using TMS (0.0 ppm) as internal standards. $^{13}C$ NMR spectra were recorded at 125.7 MHz and 150.9 MHz respectively, TMS (0.0 ppm) as an internal standard. $^{31}P$ NMR spectra were recorded at 202.5 MHz. Chemical shifts ($\delta$) are reported in ppm. MALDI-TOF mass spectra were recorded in positive ion mode. All compounds were spectroscopically pure and their structural determinations were based upon $^{1}H$ NMR, $^{13}C$ NMR, COSY, HETCORR experiments as well as by MALDI-TOF mass spectrometry.

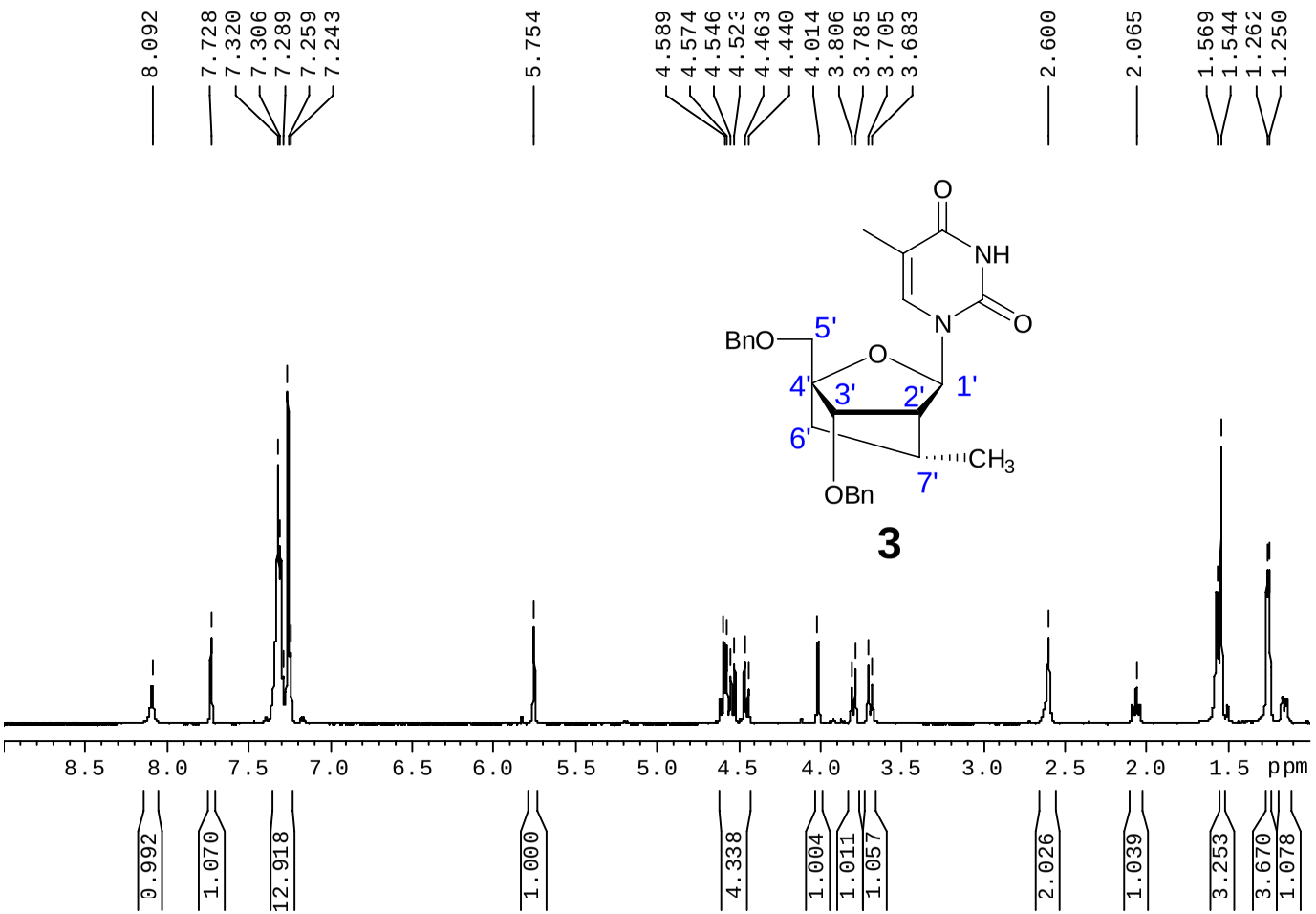


**Figure S1. 1H NMR spcetrum of compound 3.**

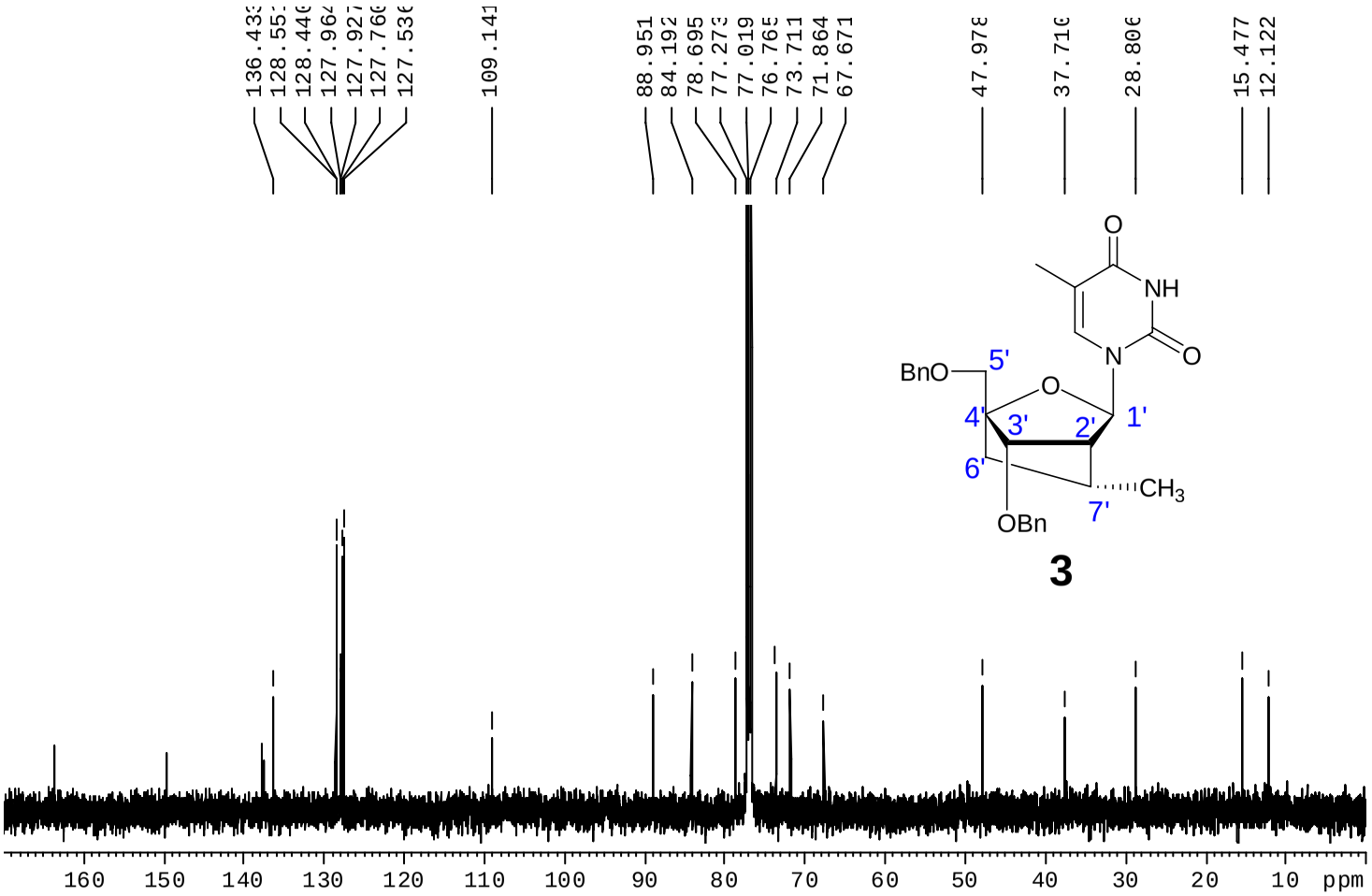


**Figure S2. $^{13}$C NMR spcetrum of compound 3.**

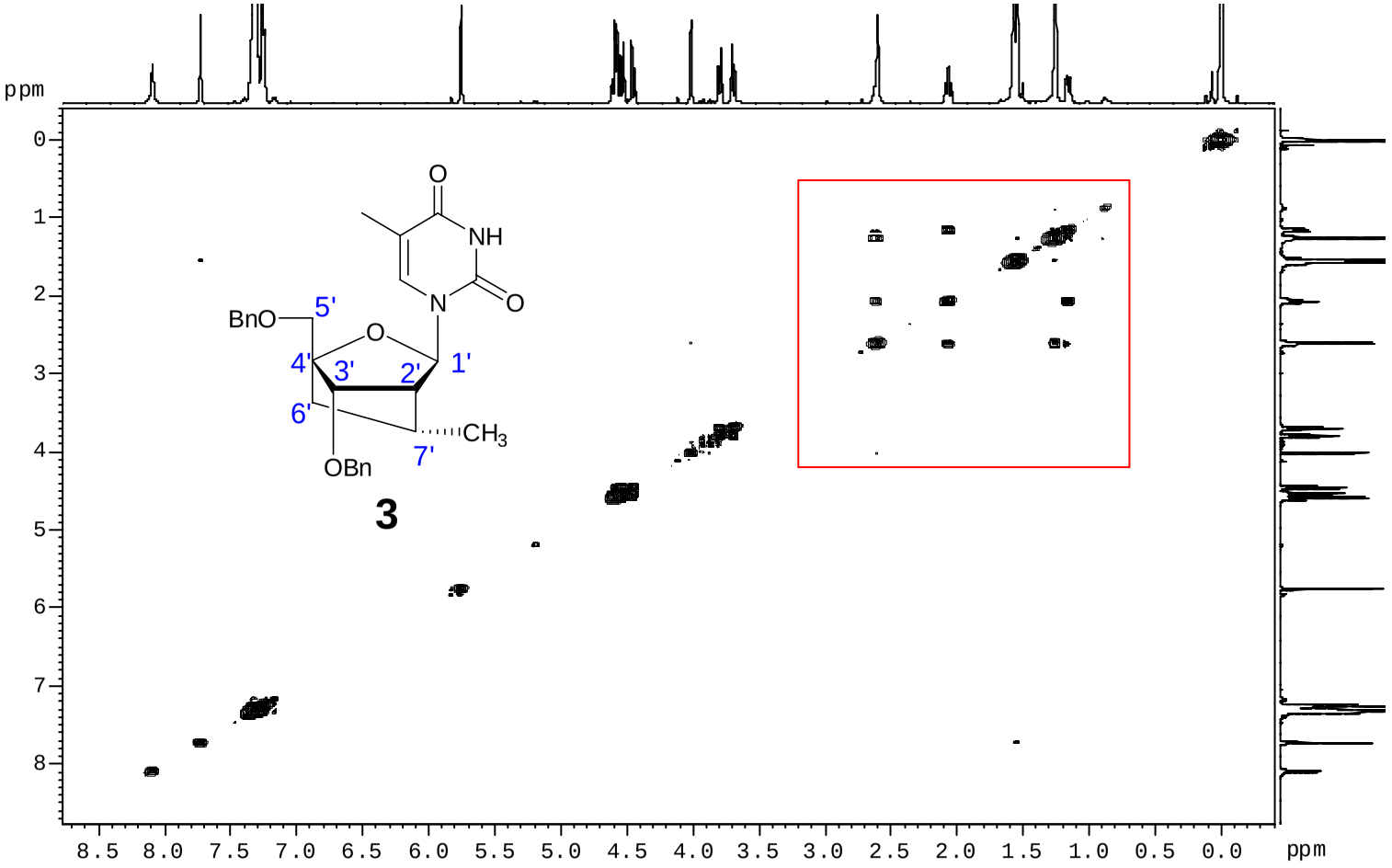


**Figure S3. COSY spcetrum of compound 3.**

The part in the red frame was expended in Figure S4.

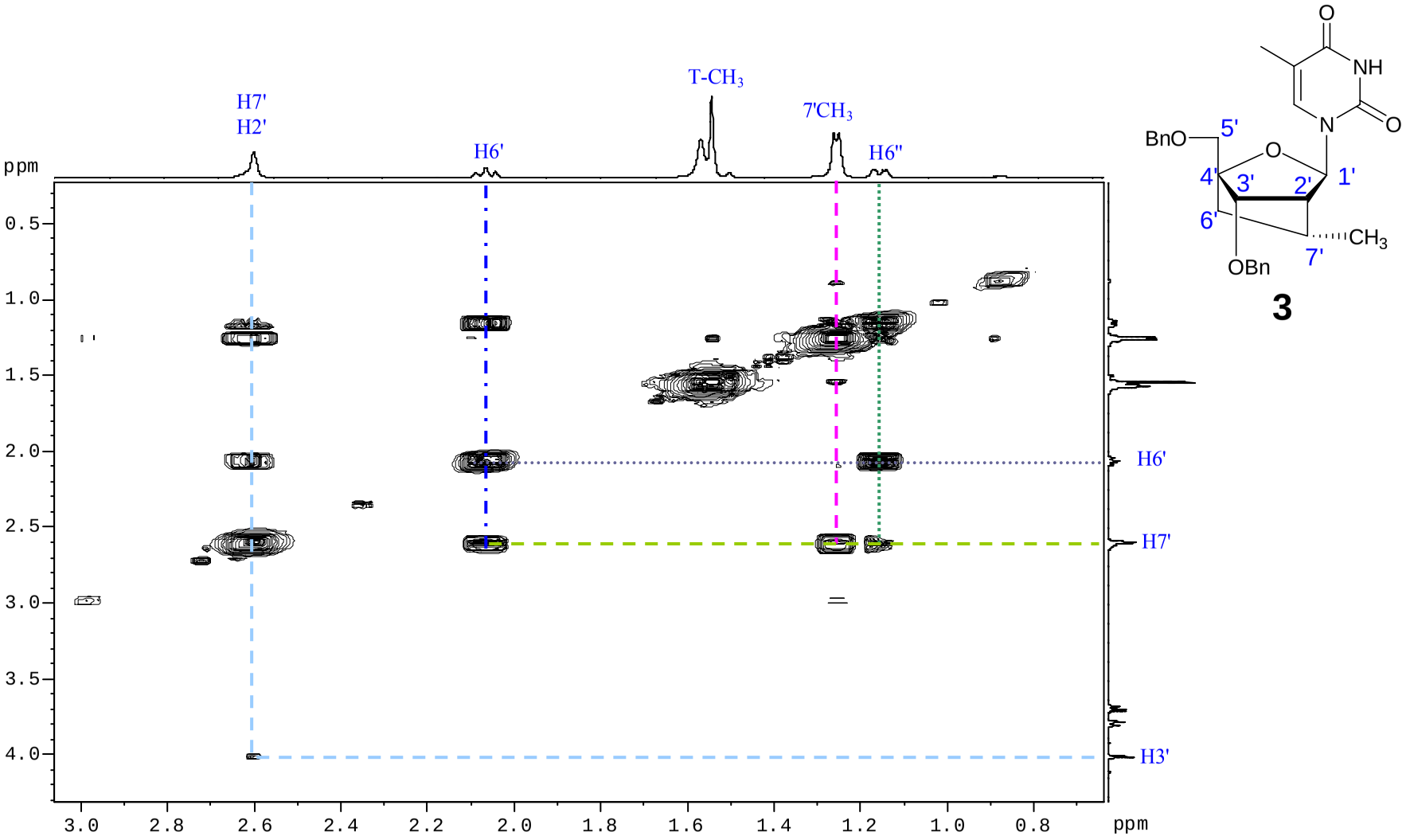


**Figure S4. Expension of COSY spcetrum of compound 3.**

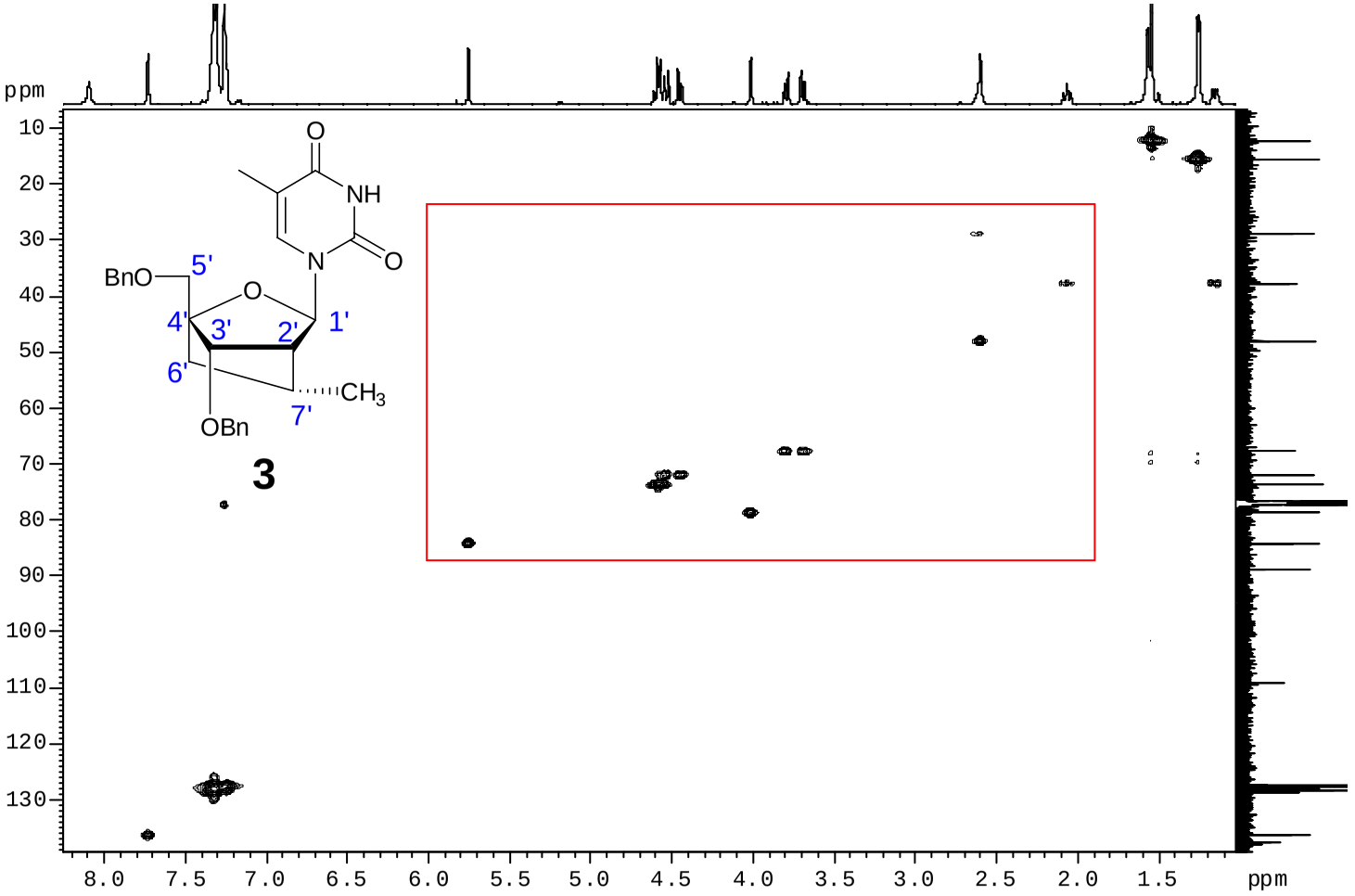


**Figure S5. HMQC spcetrum of compound 3.**

The part in the red frame was expended in Figure S6.

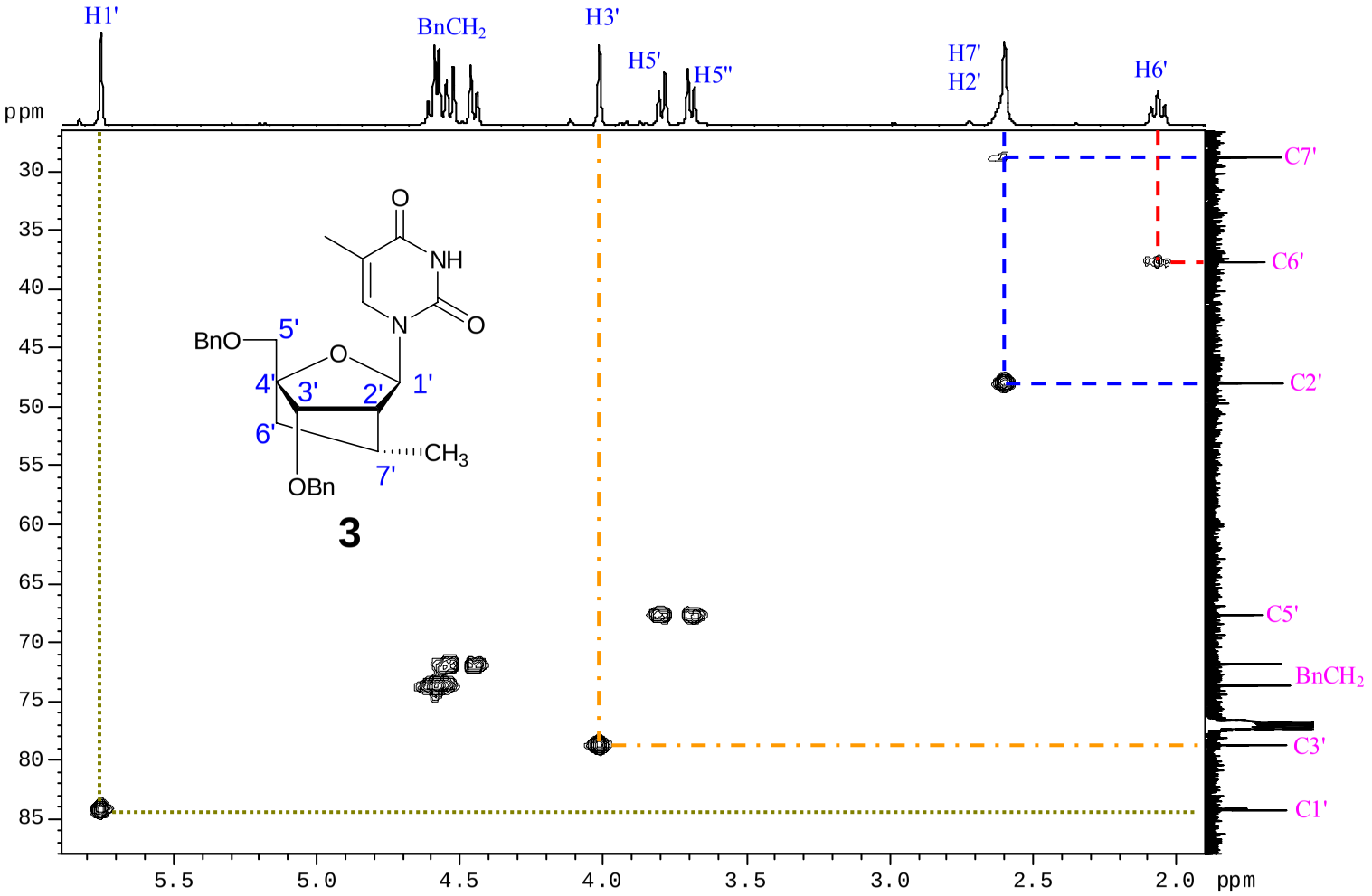


**Figure S6. Expension of HMQC spcetrum of compound 3.**

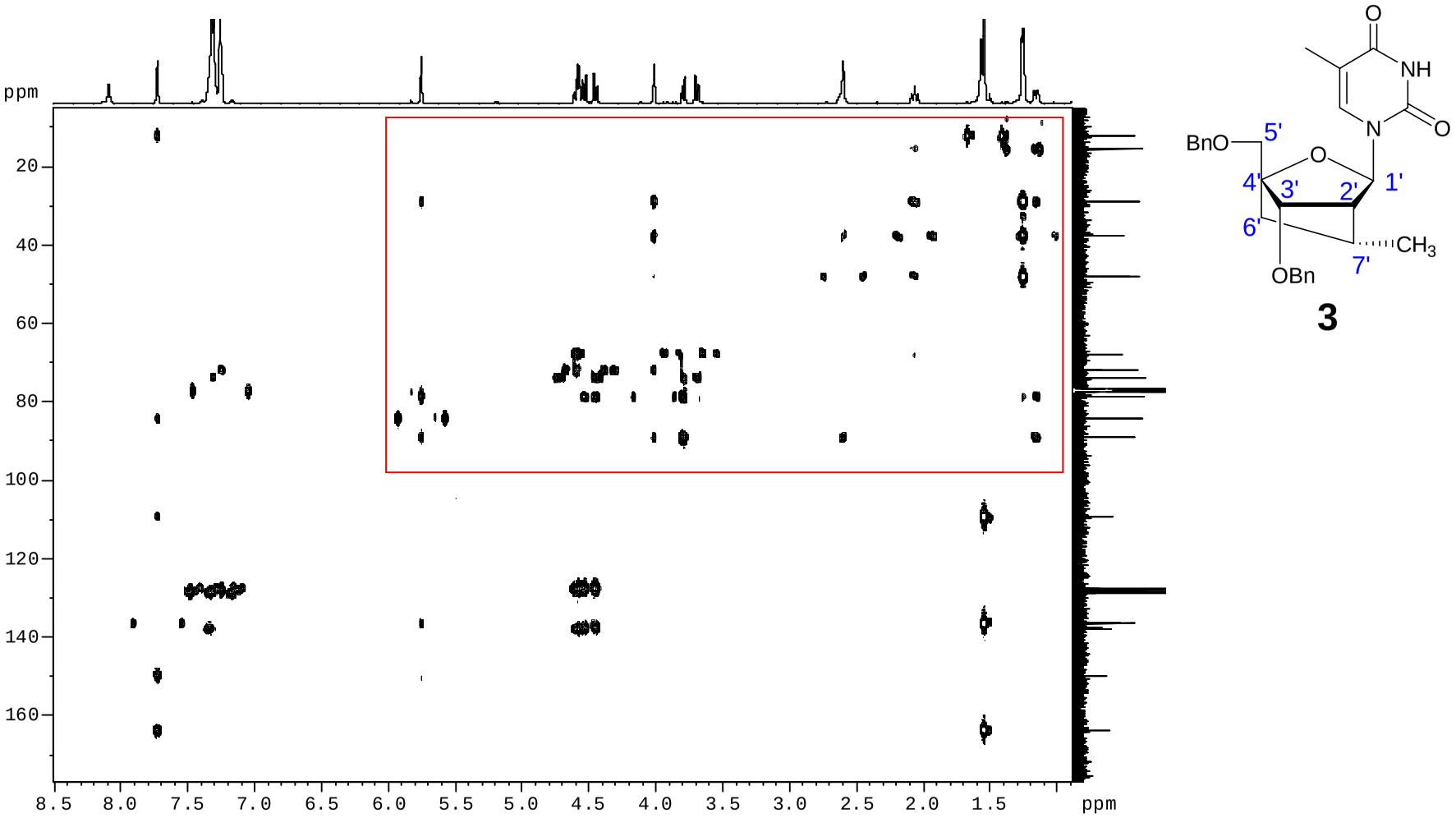


**Figure S7. HMBC spcetrum of compound 3.**

The part in the red frame was expended in Figure S8.

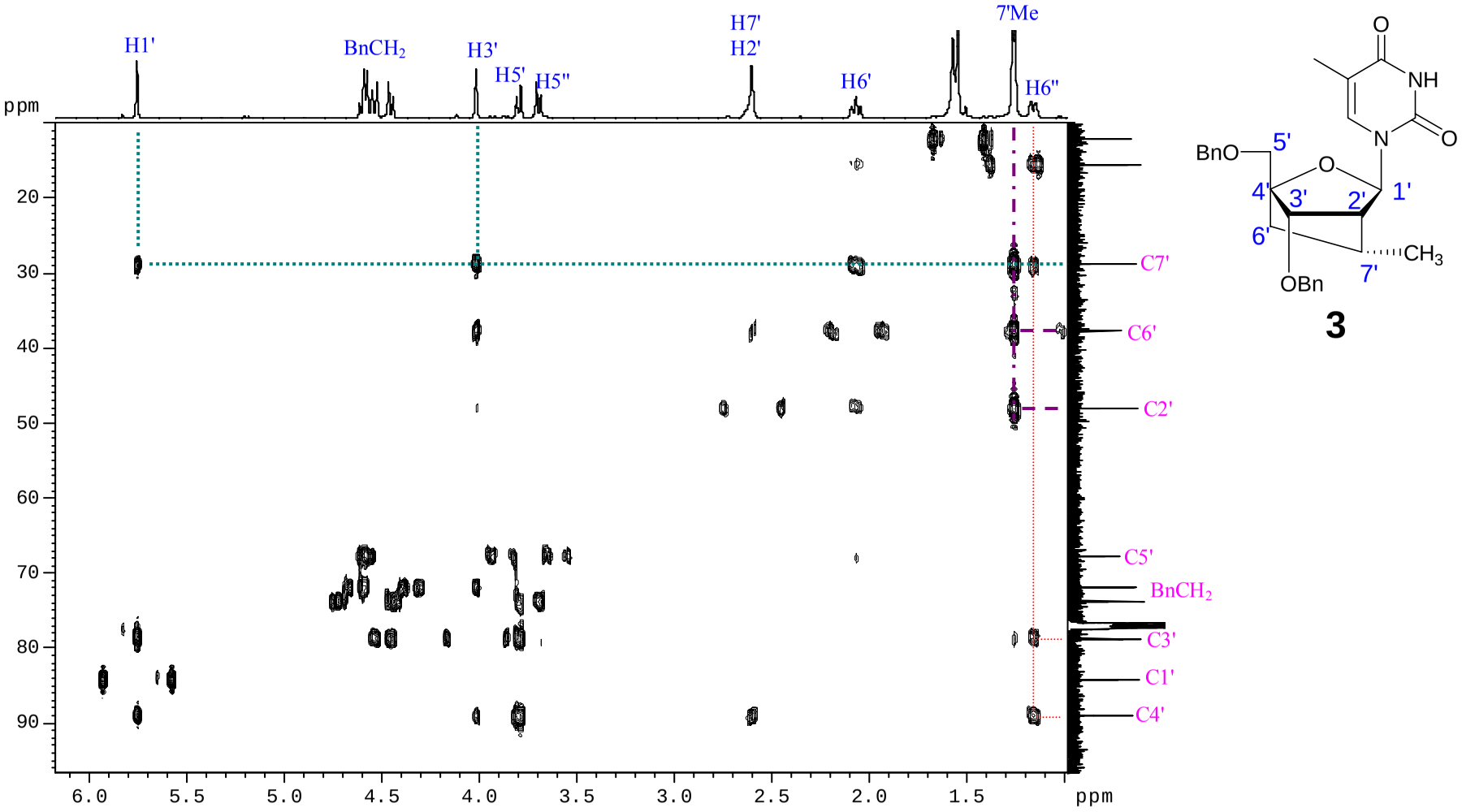


**Figure S8. Expension of HMBC spcetrum of compound 3.**

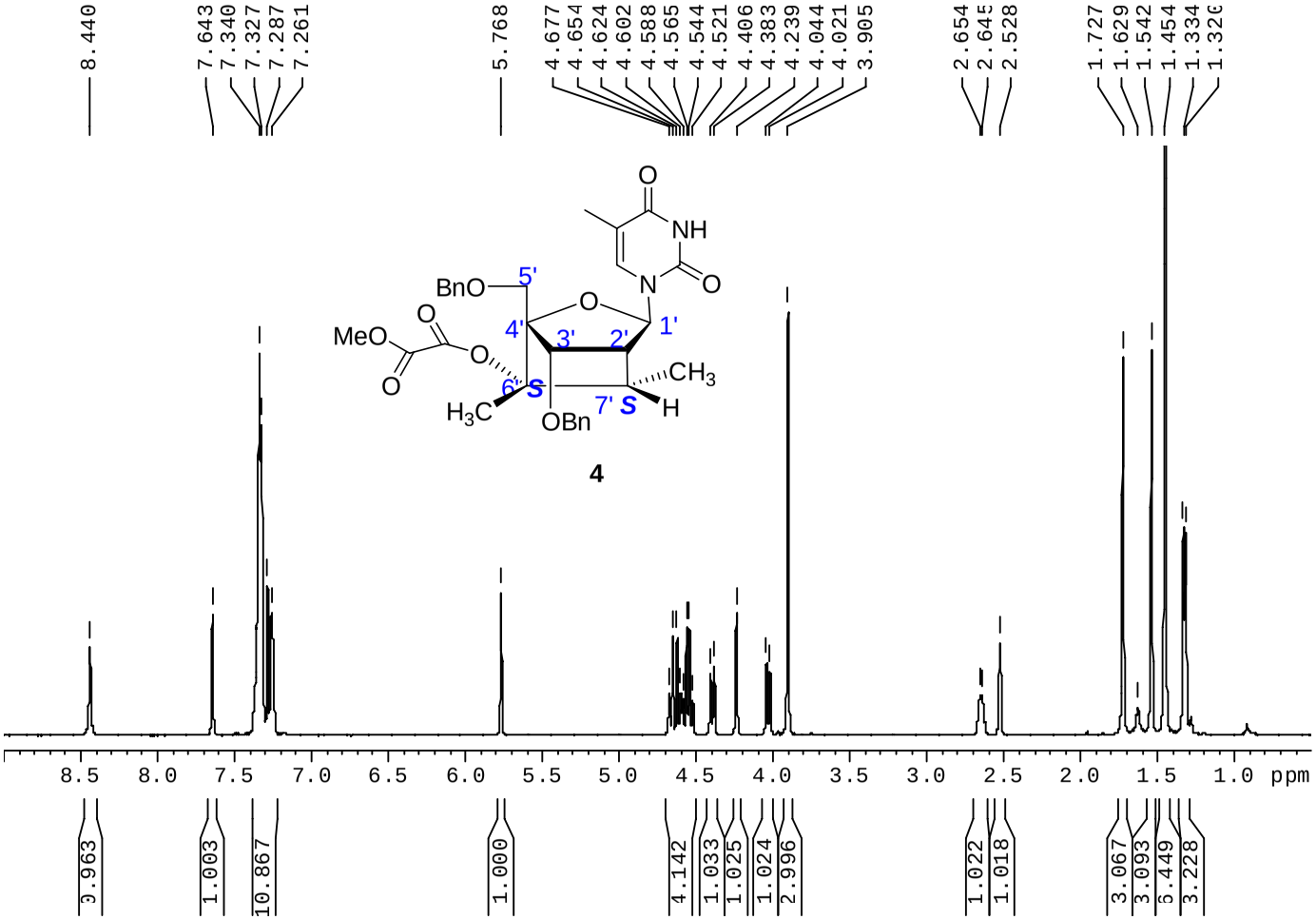


**Figure S9. $^{1}$H NMR spectrum of compound 4.**

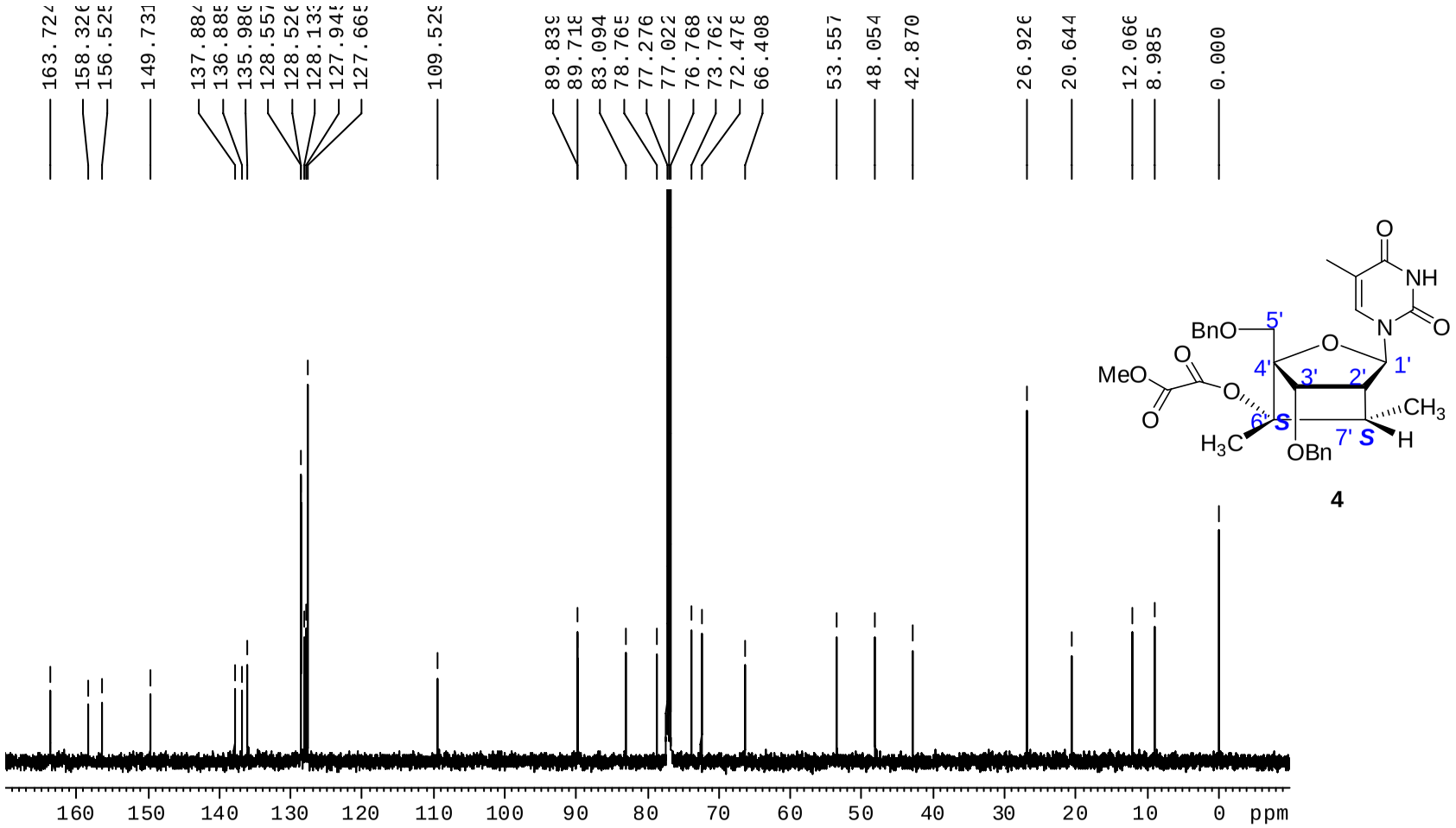


**Figure S10. $^{13}$C NMR spectrum of compound 4.**

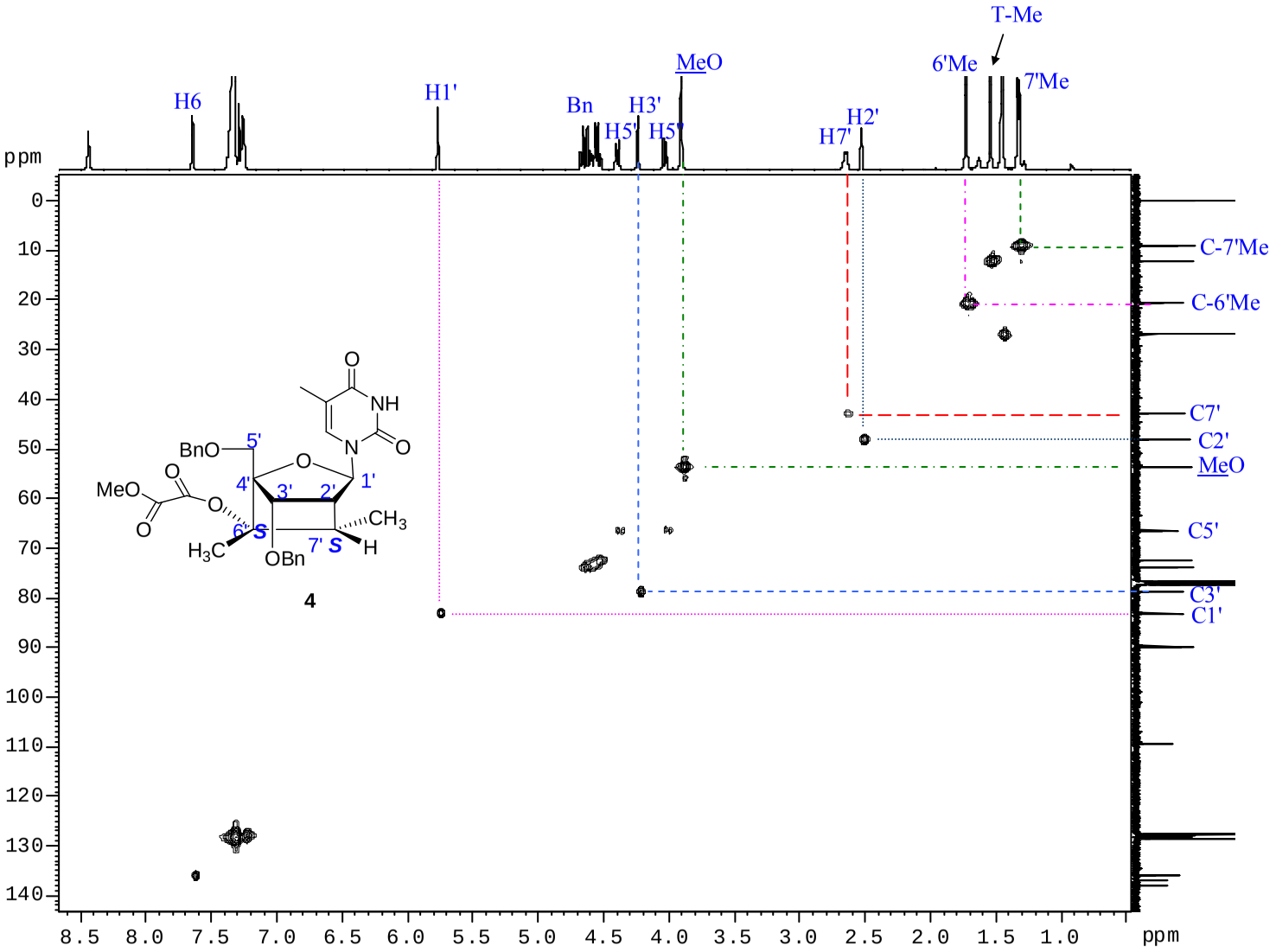


**Figure S11. HMQC spectrum of compound 4.**

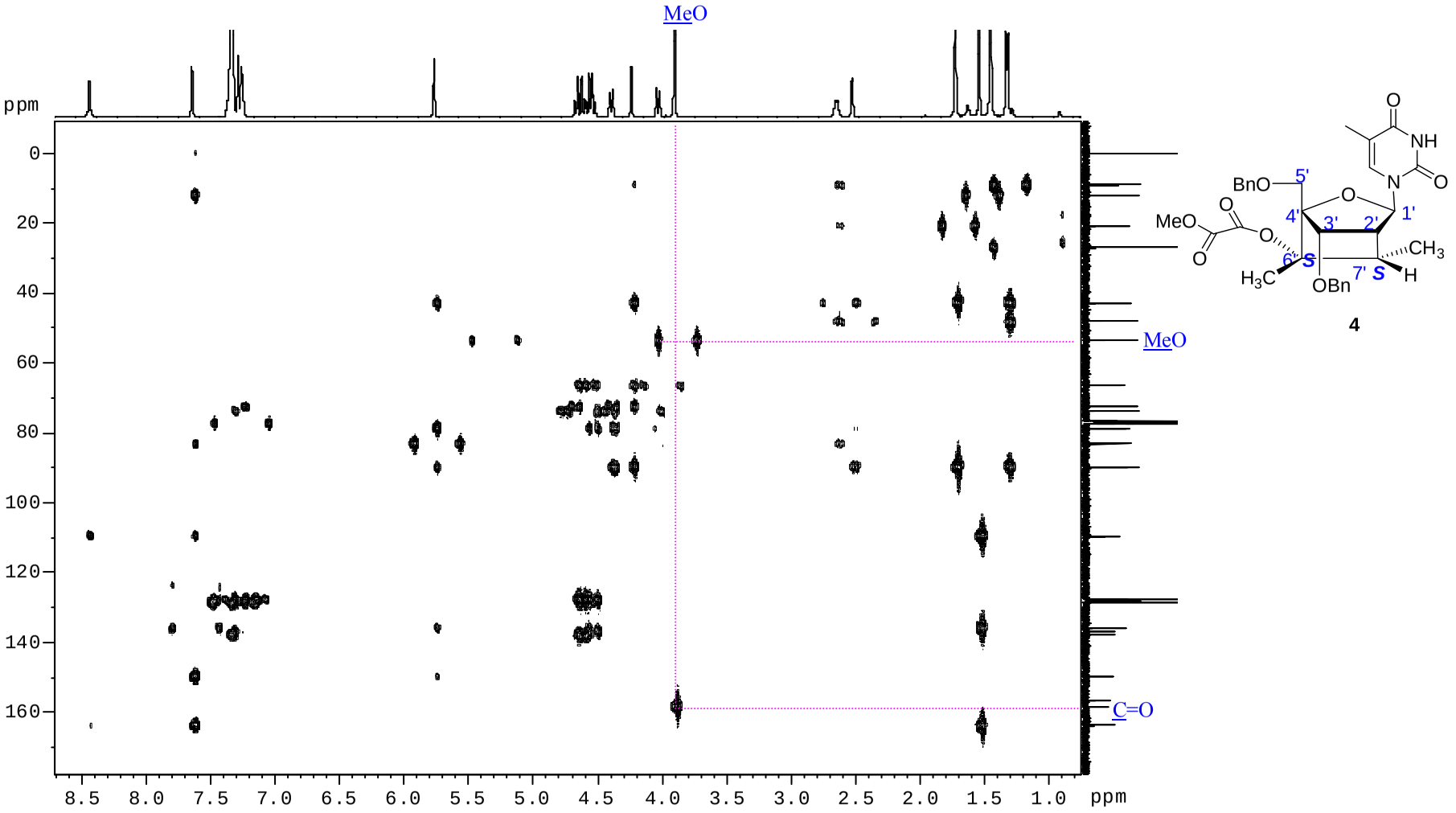


**Figure S12. HMBC spectrum of compound 4.**

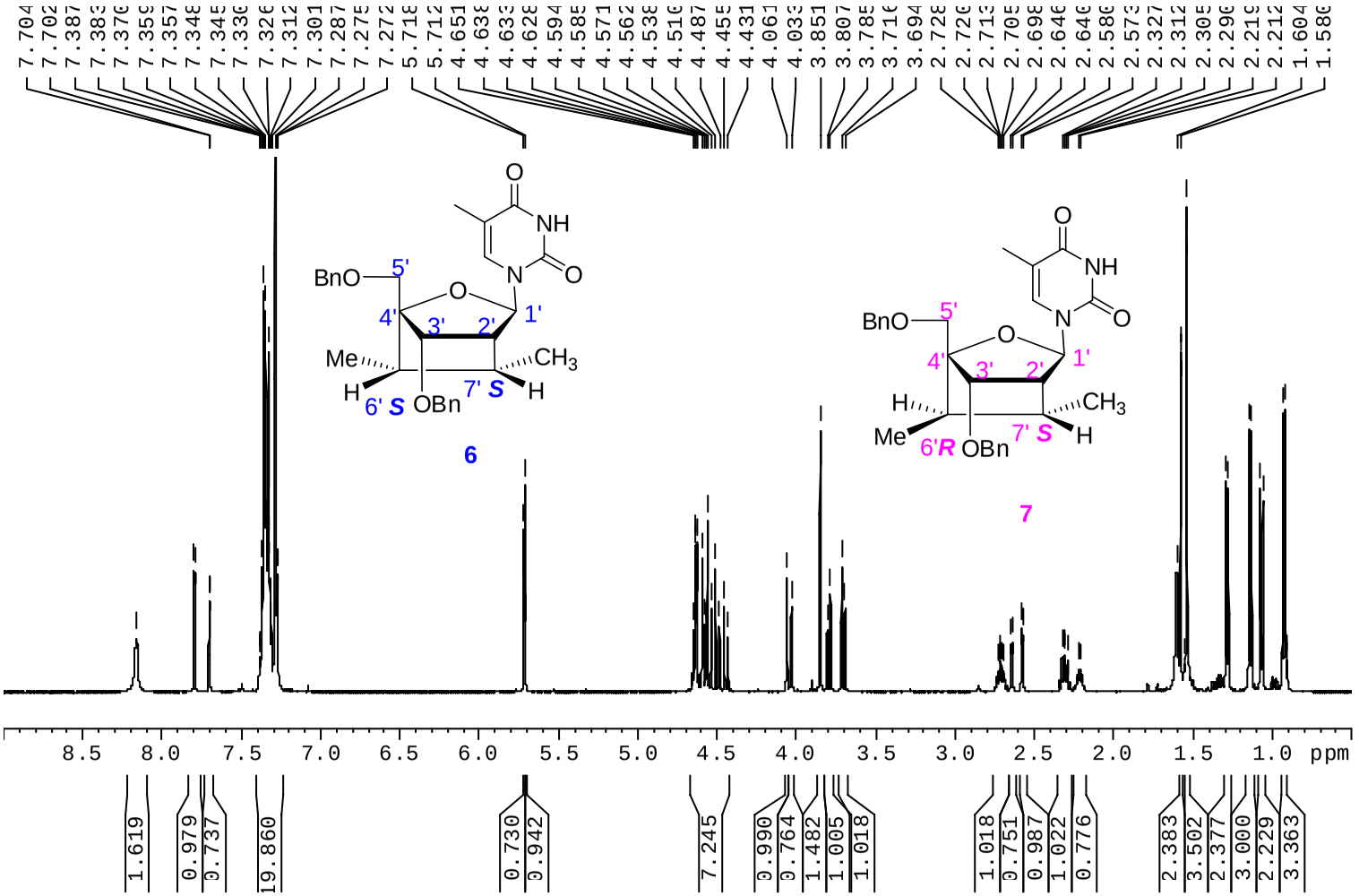


**Figure S13. $^{1}$H NMR spectrum of compound 6/7.**

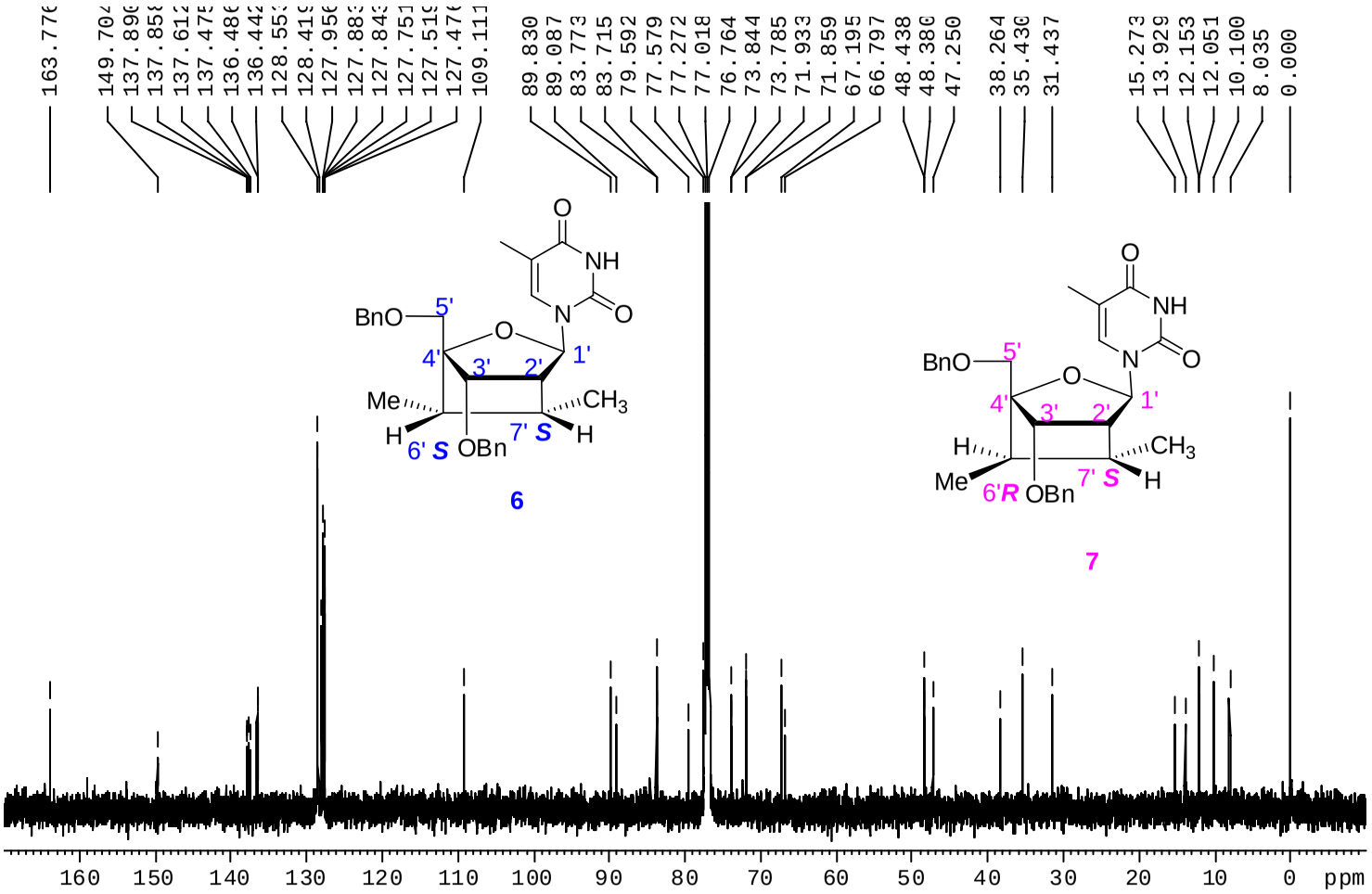


**Figure S14. $^{13}$C NMR spectrum of compound 6/7.**

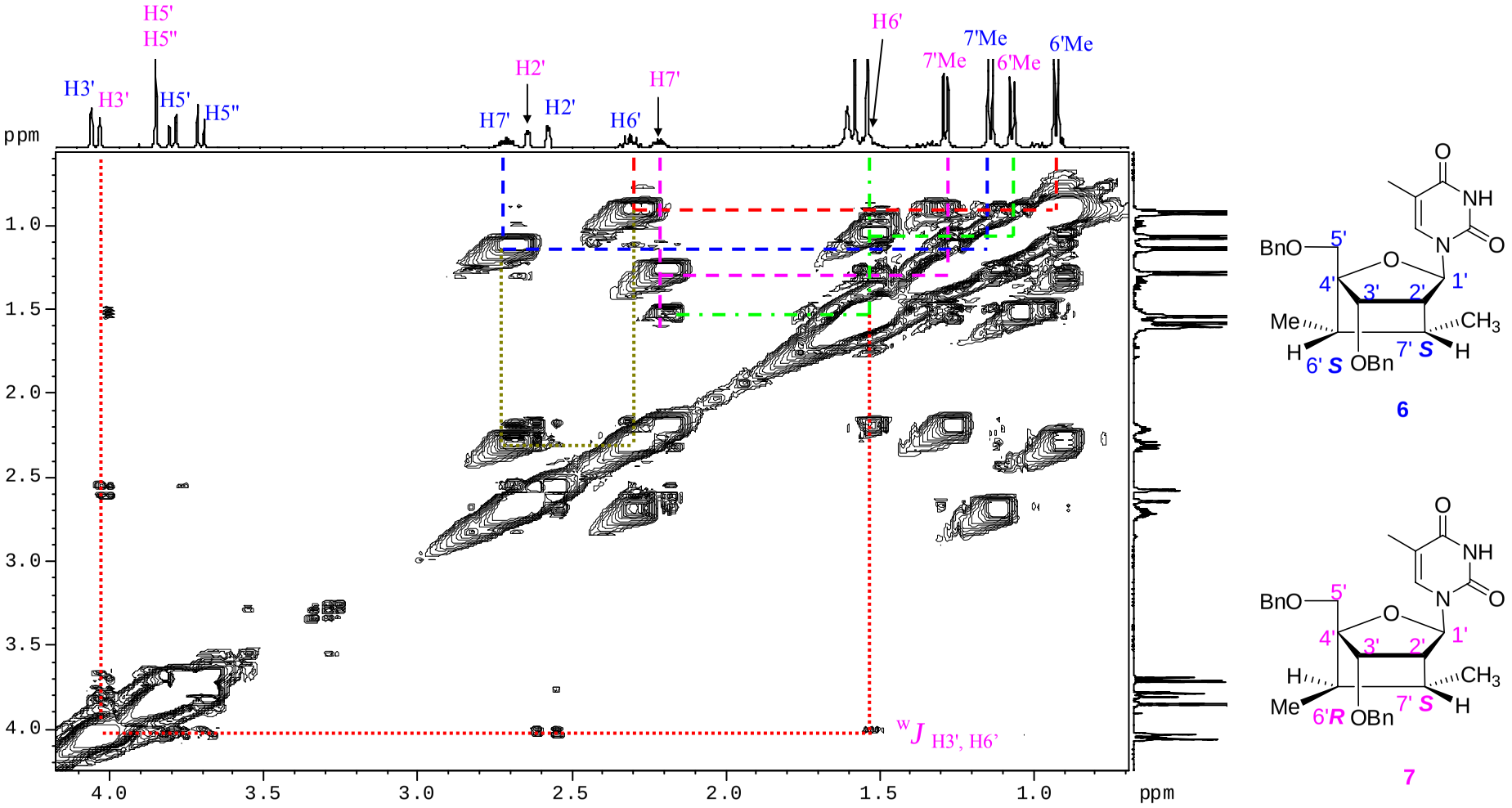


**Figure S15. COSY spectrum of compound 6/7.**

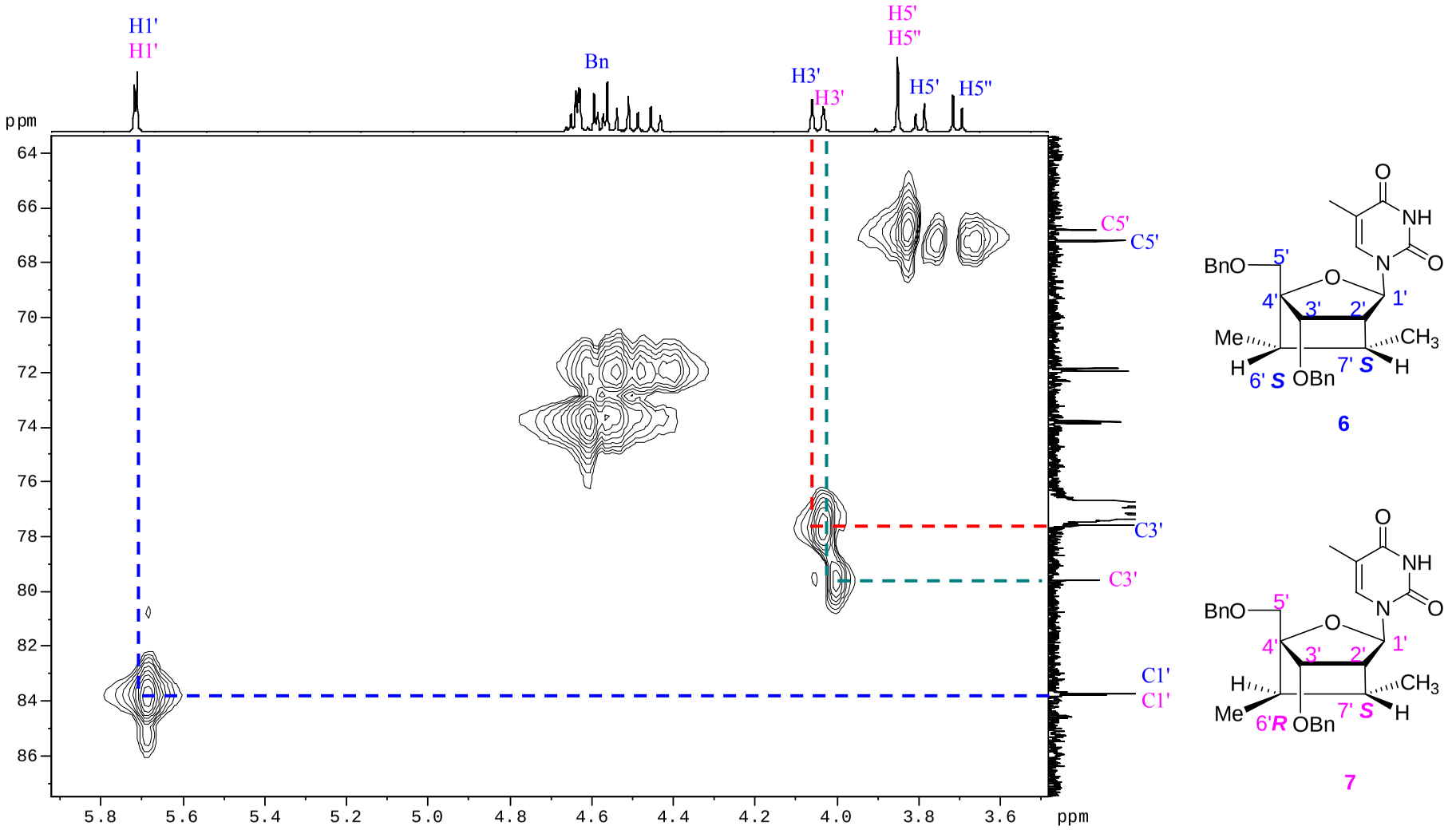


**Figure S16. HMQC spectrum of compound 6/7.**

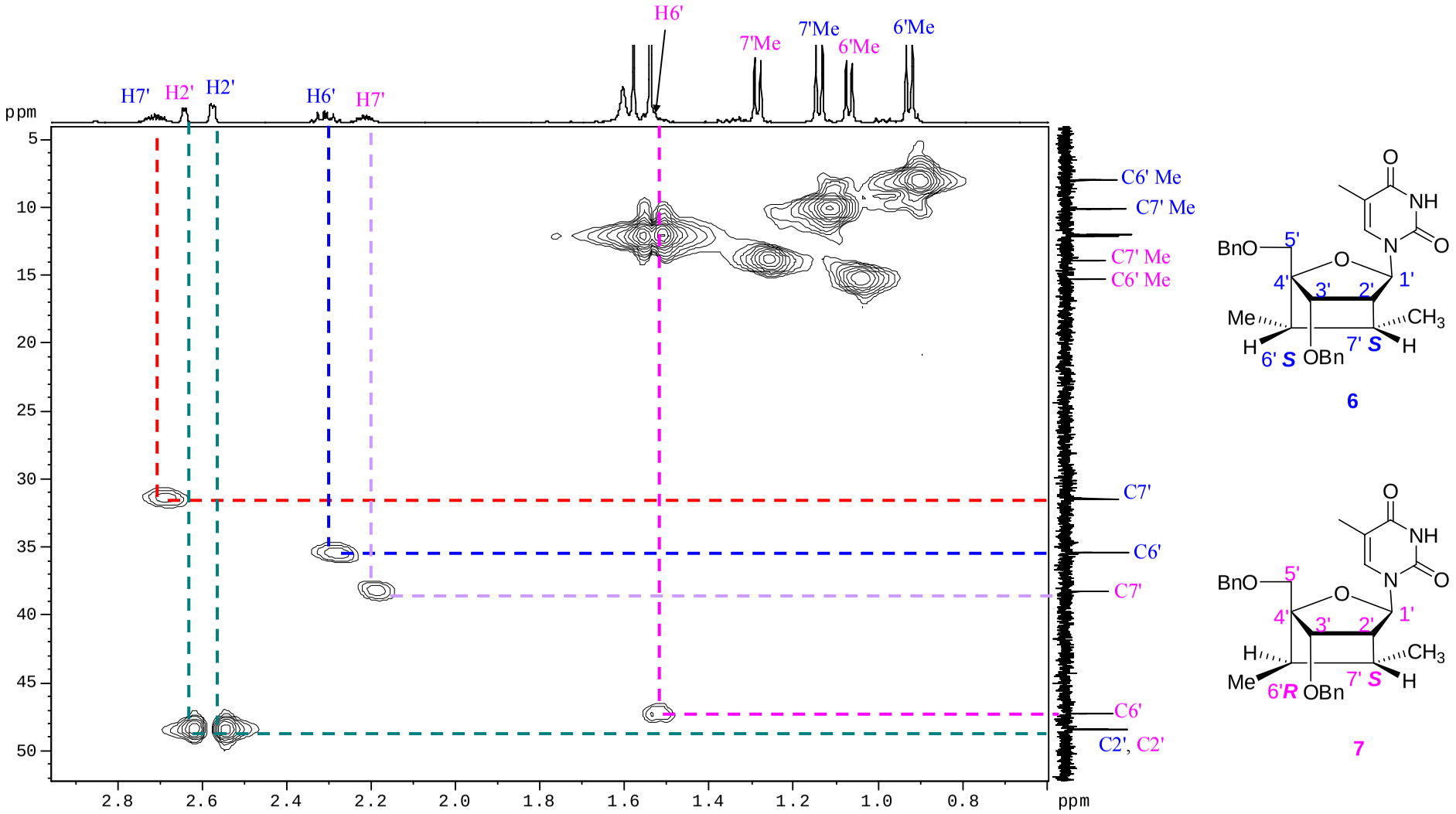


**Figure S17. HMQC spectrum of compound 6/7.**

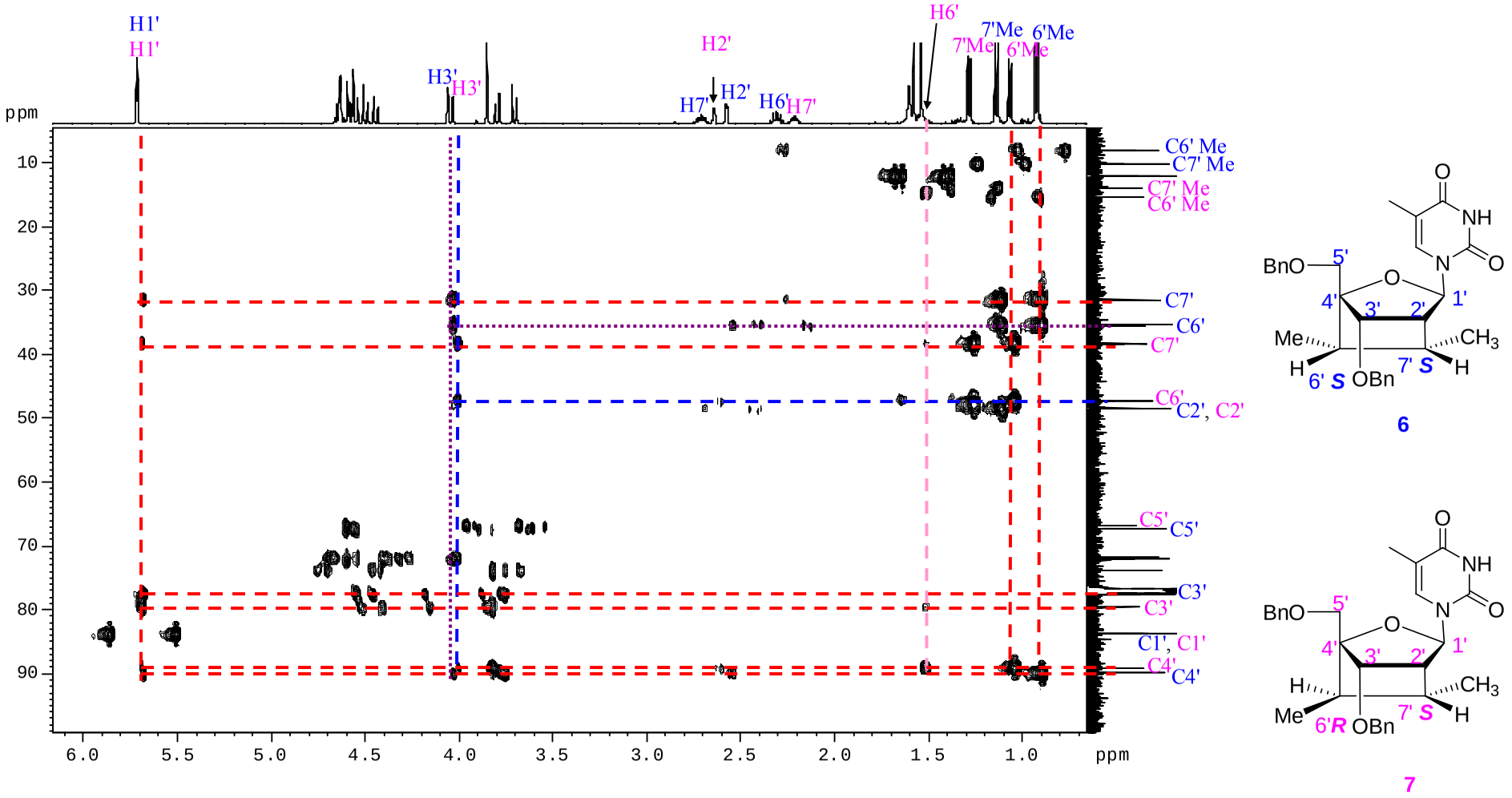


**Figure S18. HMBC spectrum of compound 6/7.**

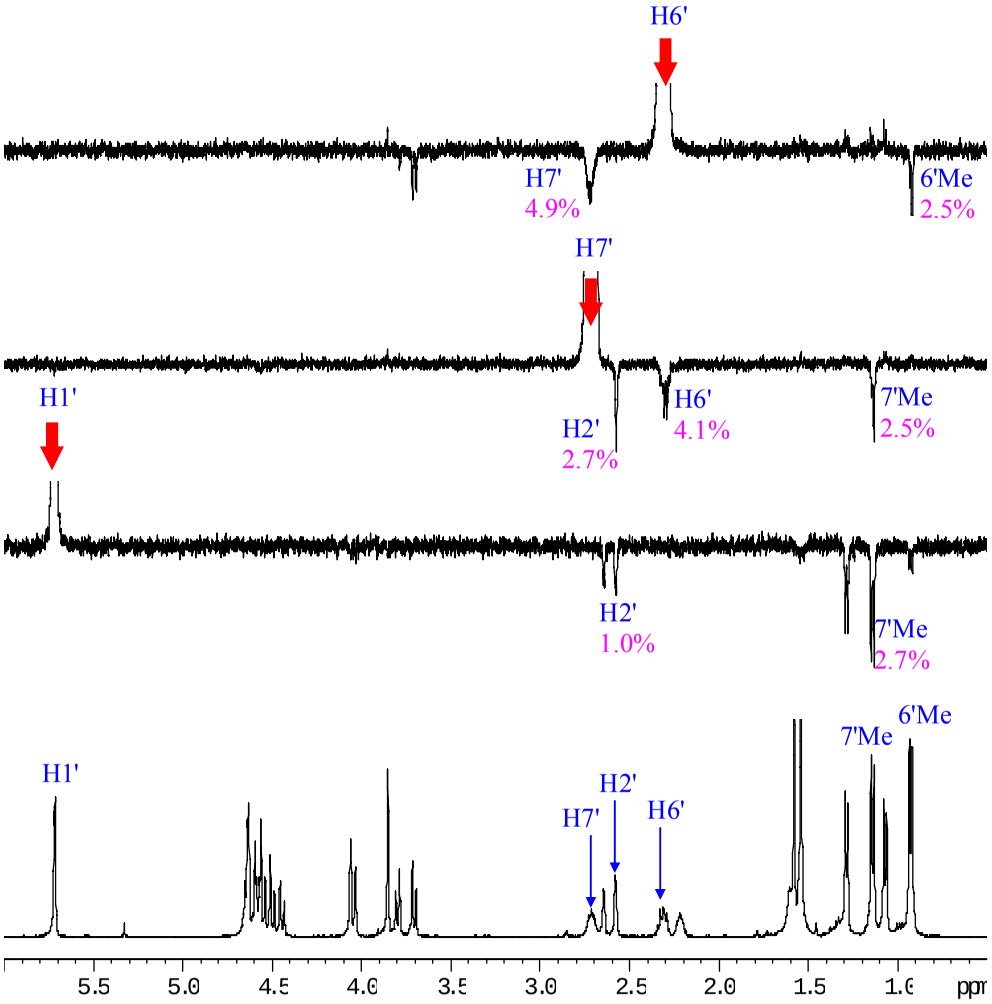


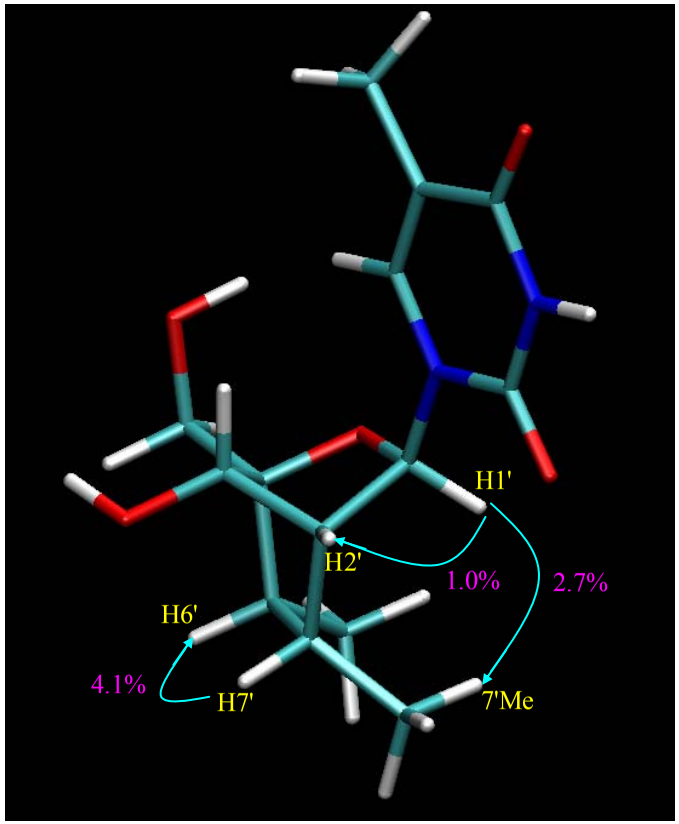


**Figure S19. 1D nOe specturm of compound 6.**

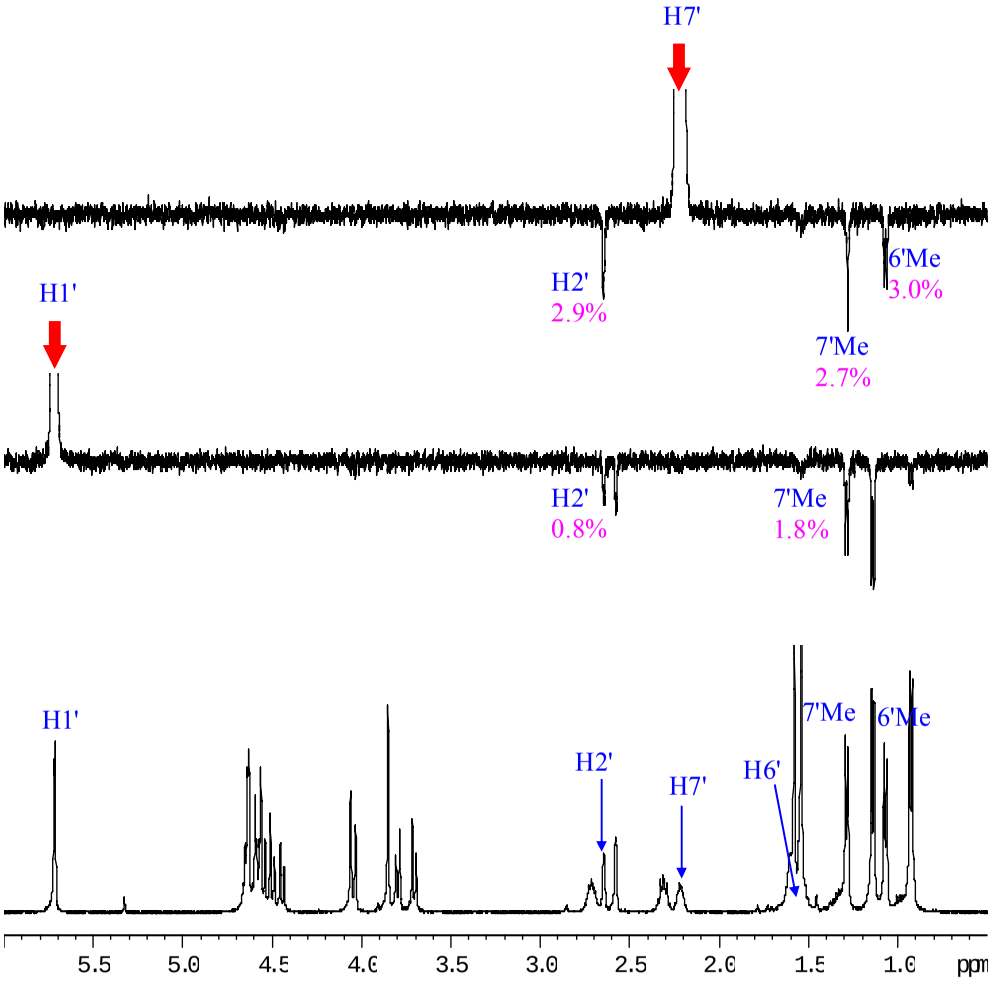


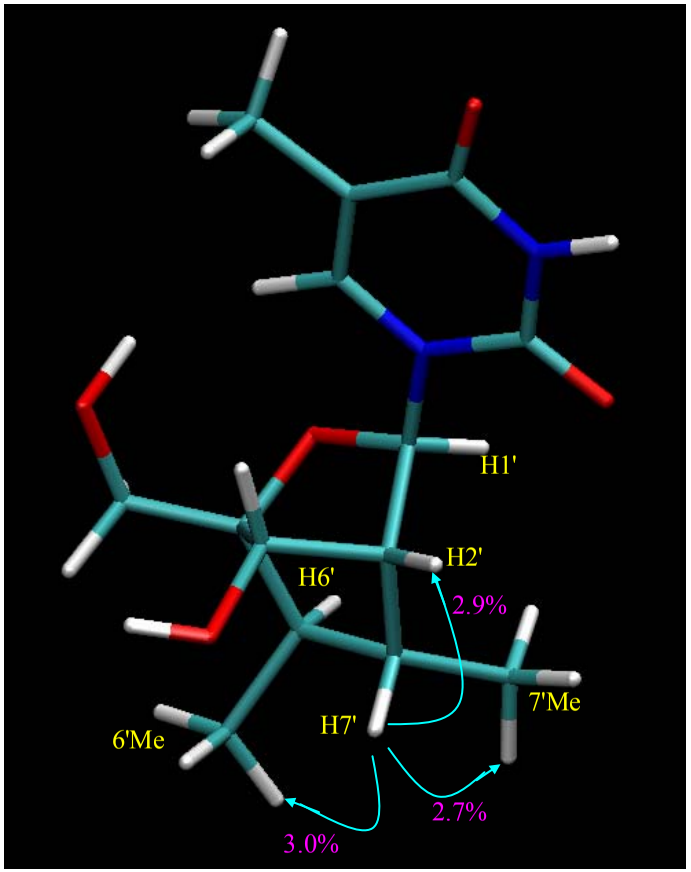


**Figure S20. 1D nOe specturm of compound 7.**

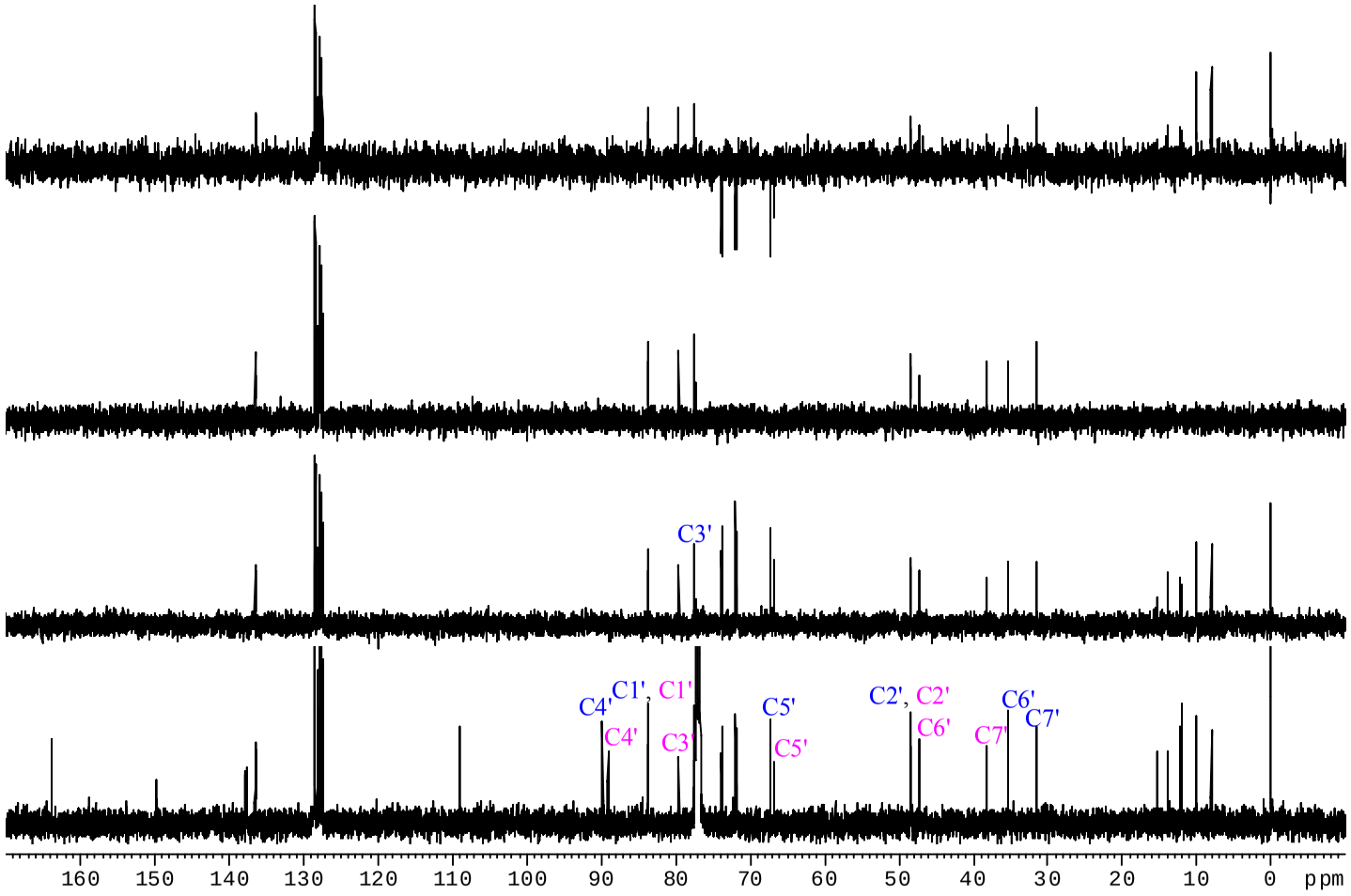


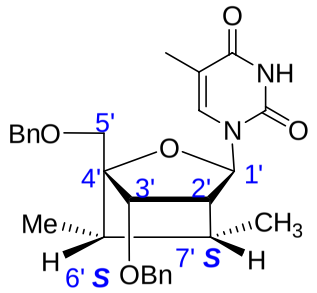


**6**

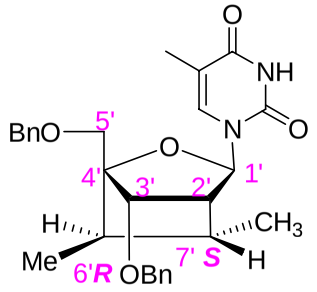


**7**

**Figure S21. DEPT specturm of compound 6 and 7.**

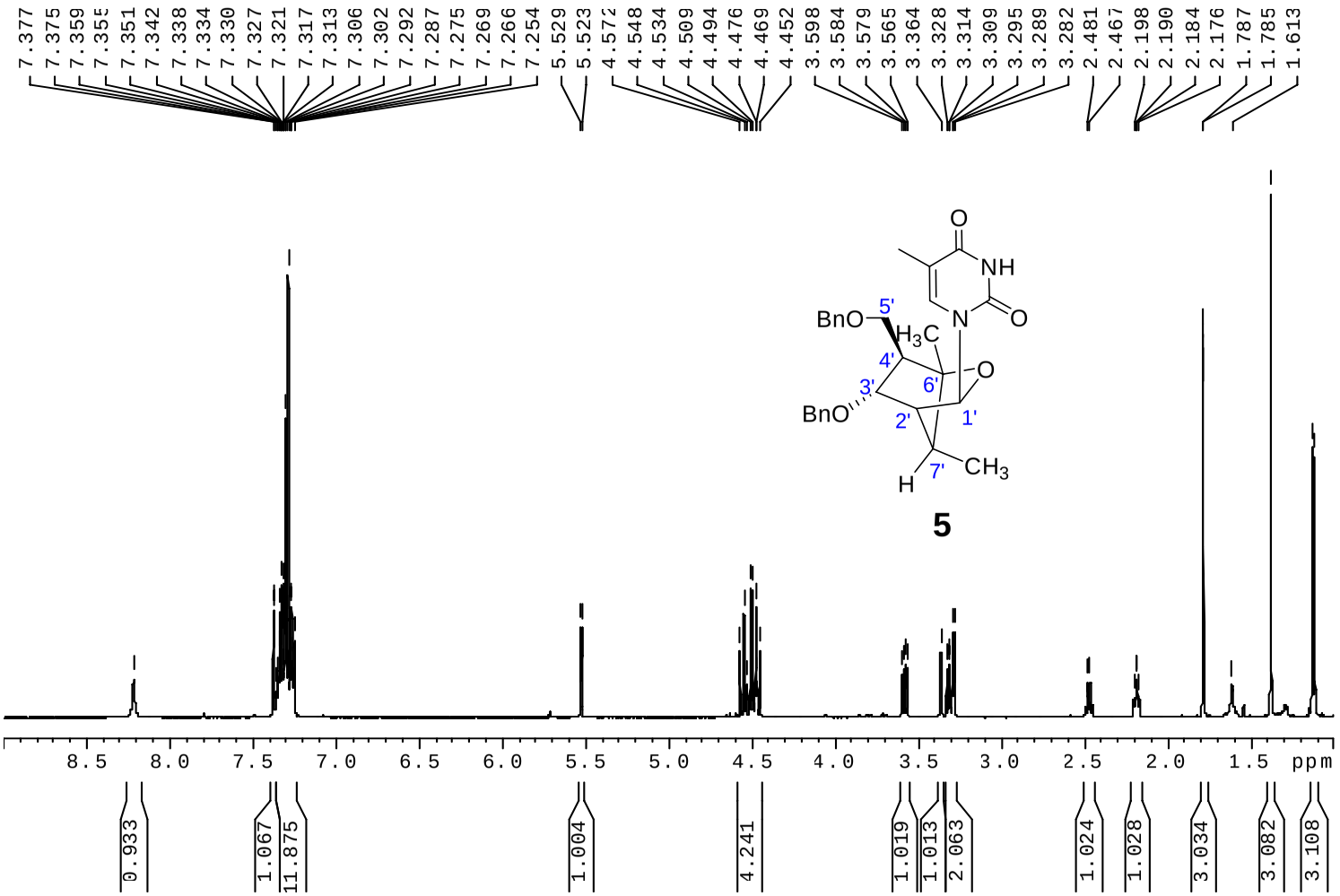


**Figure S22. $^{1}$H NMR spectrum of compound 5.**

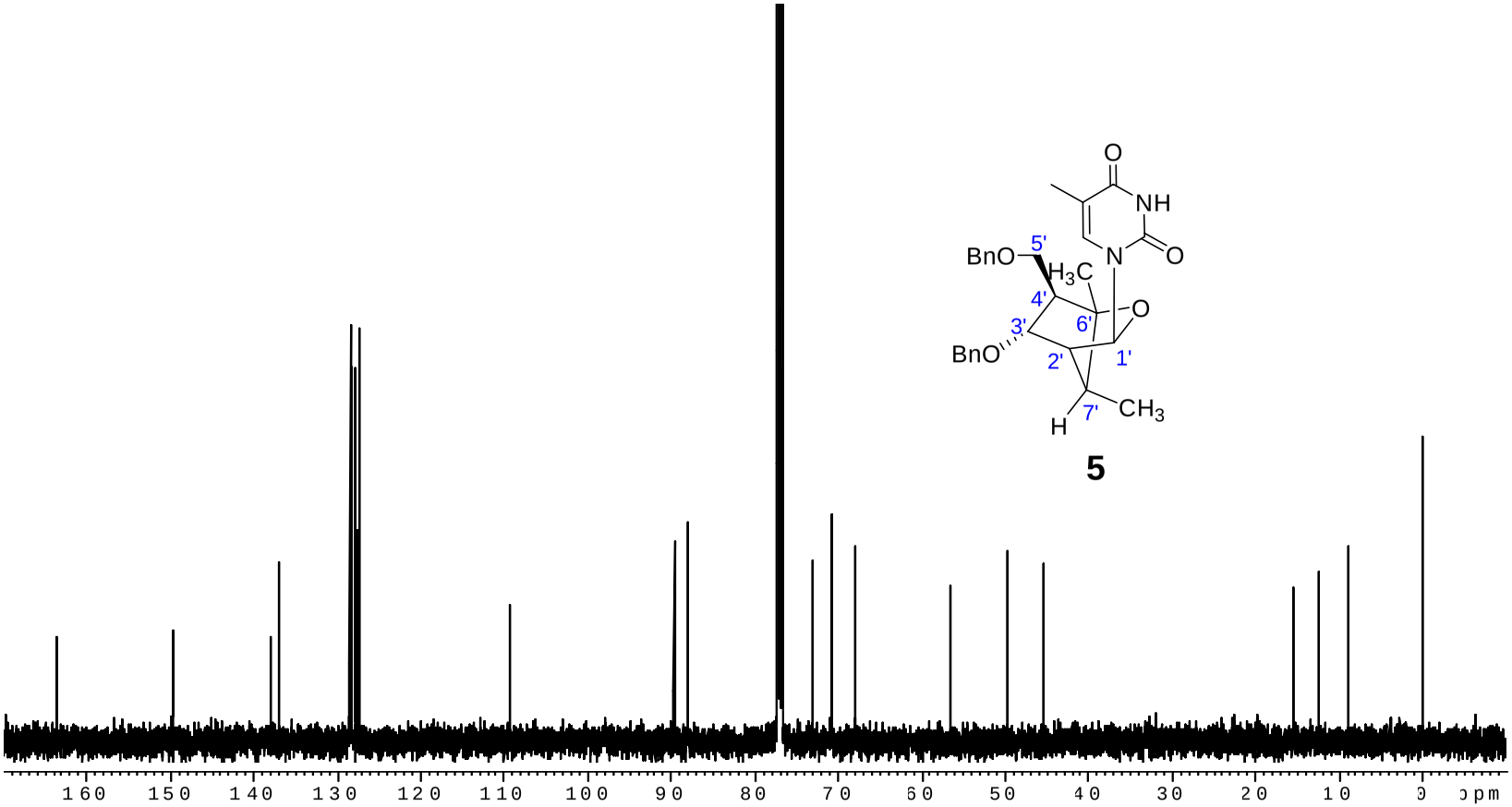


**5**

**Figure S23. $^{13}$C NMR spectrum of compound 5.**

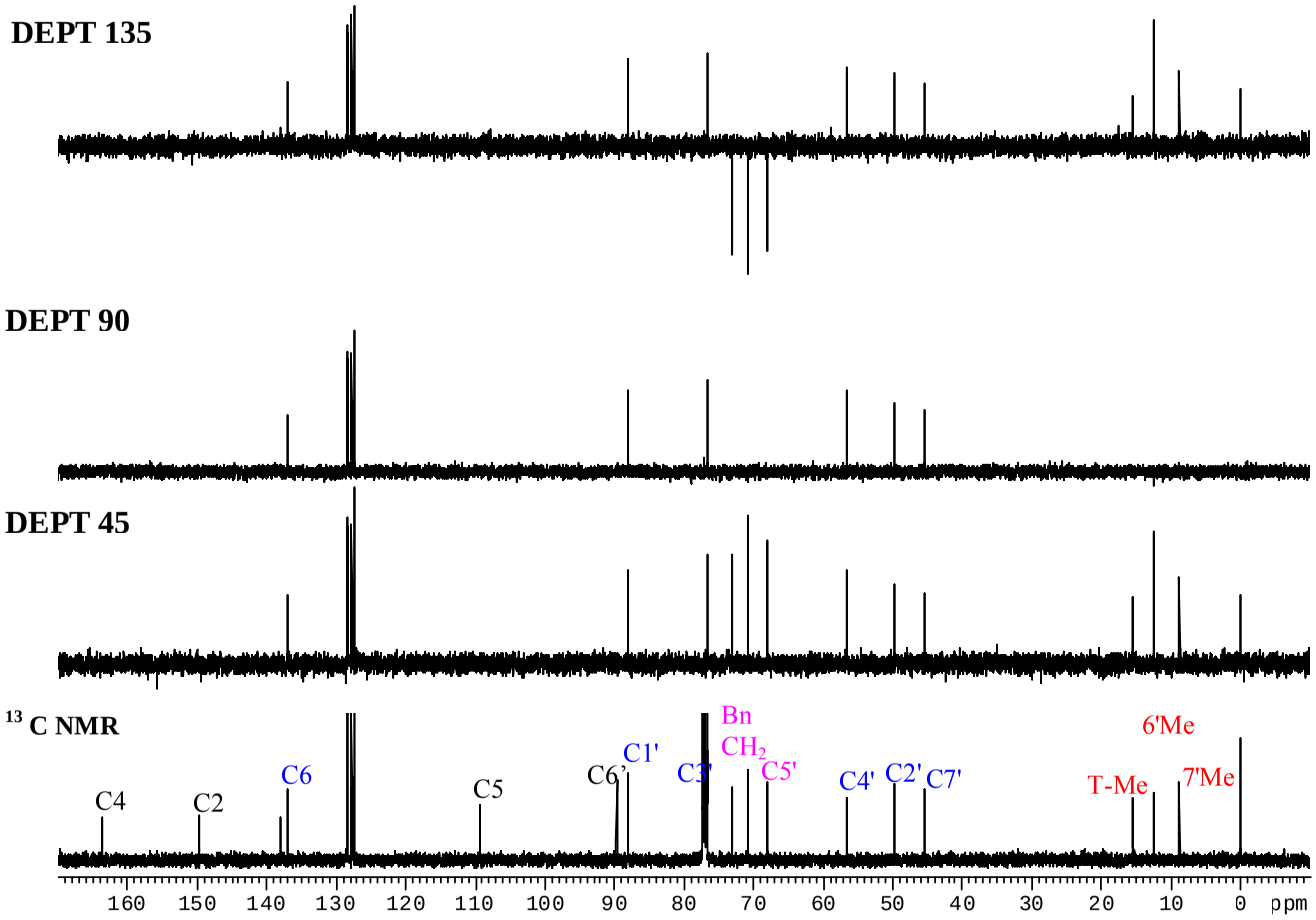


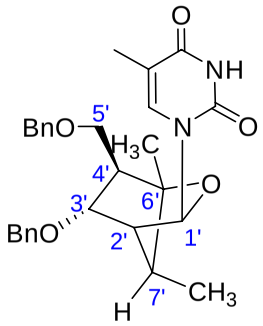


**5**

**Figure S24. DEPT spectra of compound 5.**

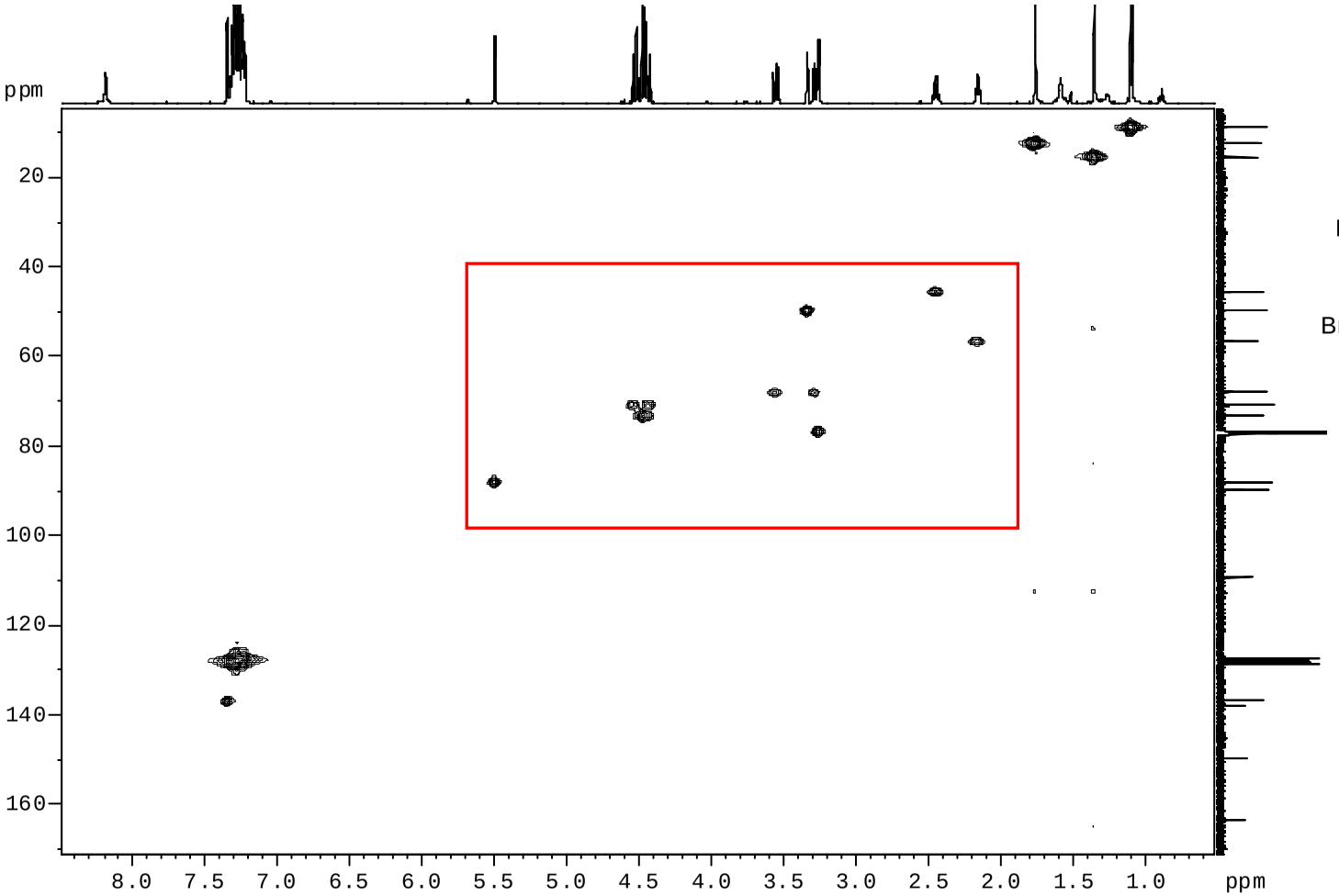


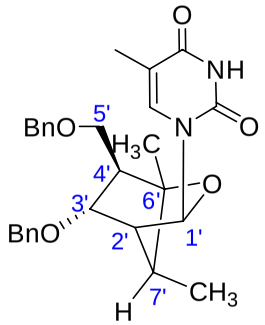


**5**

**Figure S25.** $^{1}H$-$^{13}C$ **HMQC spectra of product 5.**

The part inside the red frame was expended in Figure s26.

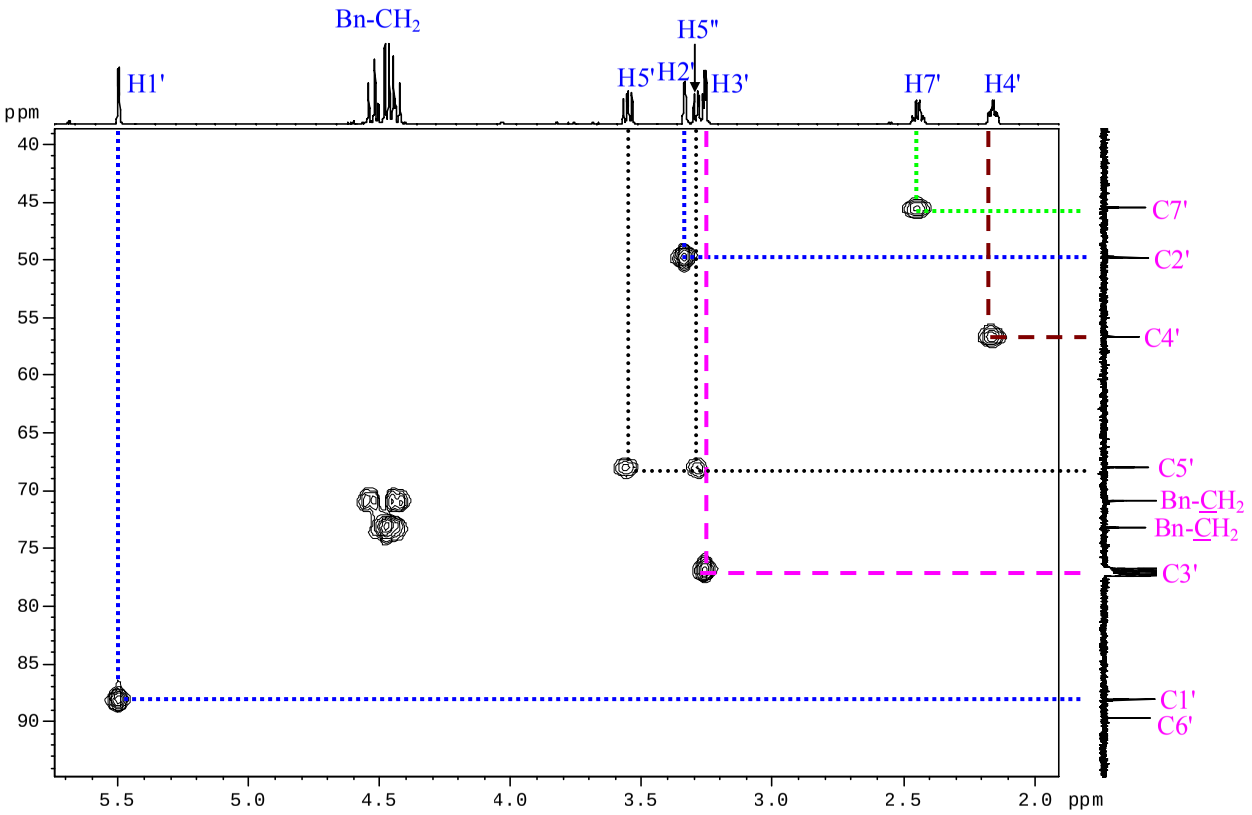


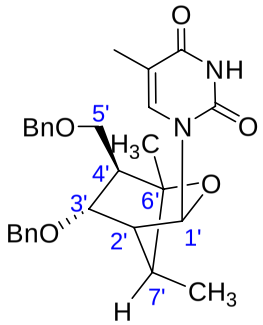


**5**

**Figure S26. Expension of $^{1}$H-$^{13}$C HMQC spectra of product 5.**

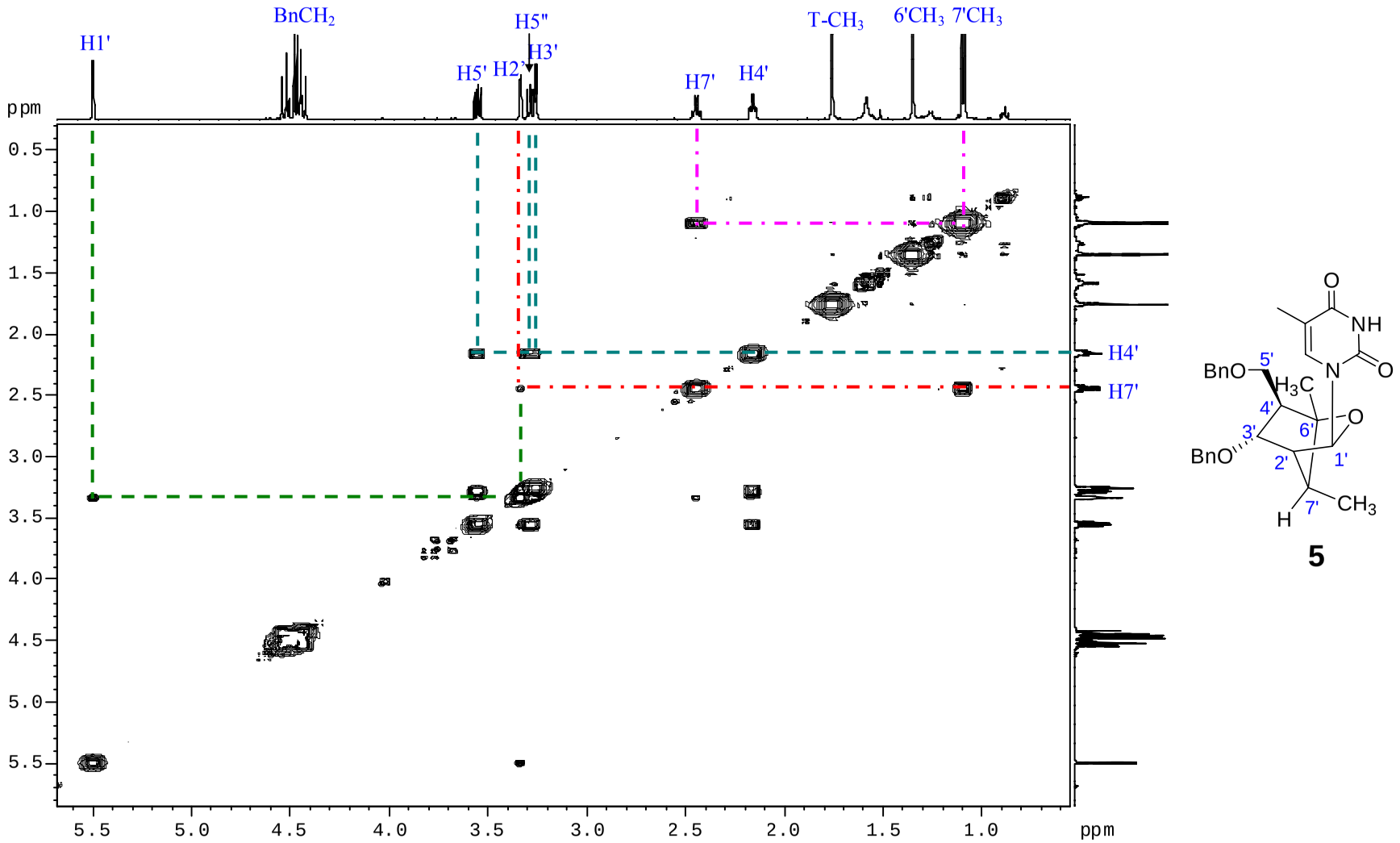


**Figure S27. COSY spectra of compound 5.**

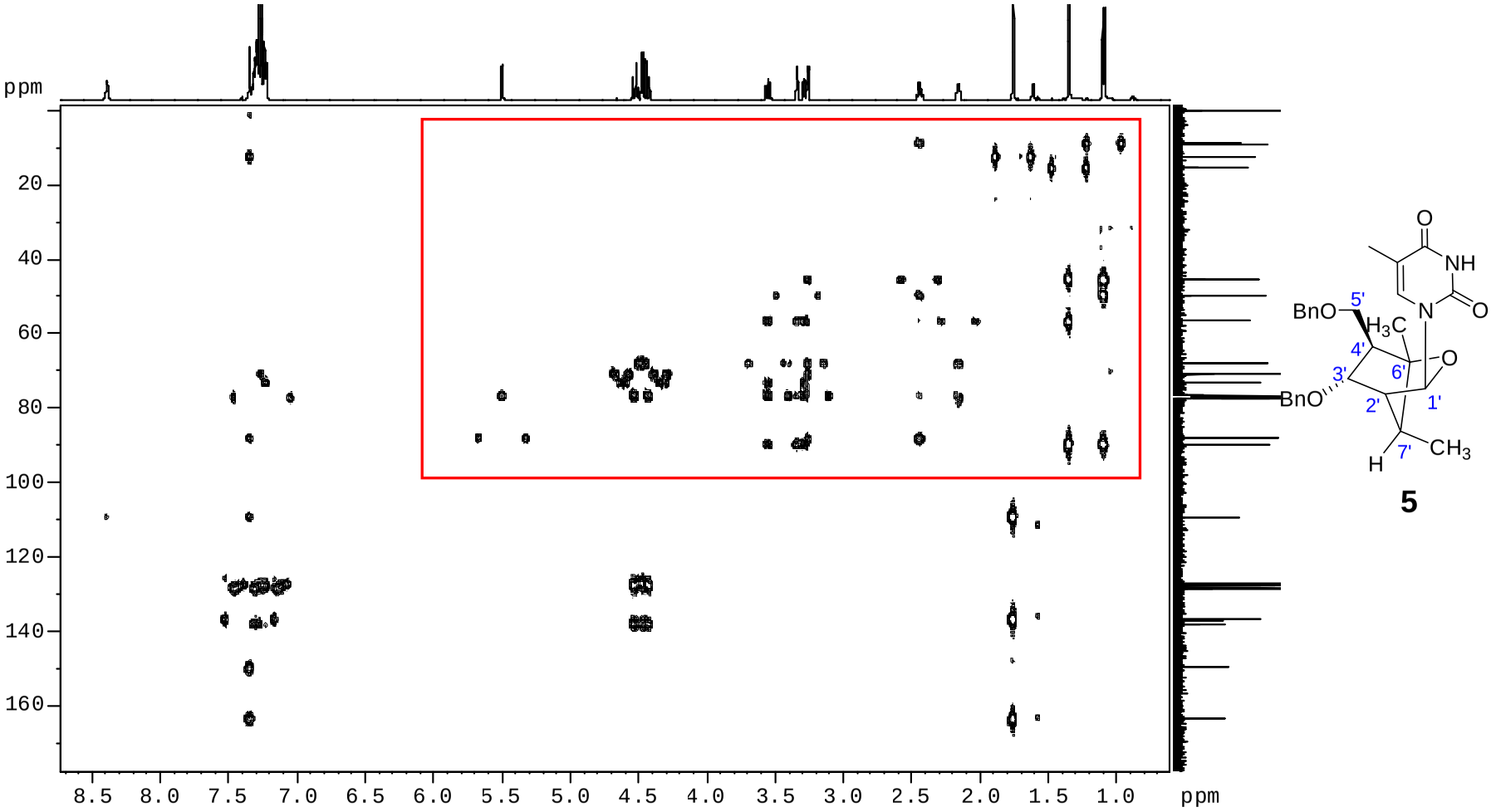


**Figure S28. HMBC spectra of compound 5.**

The part inside the red frame was expended in Figure S29.

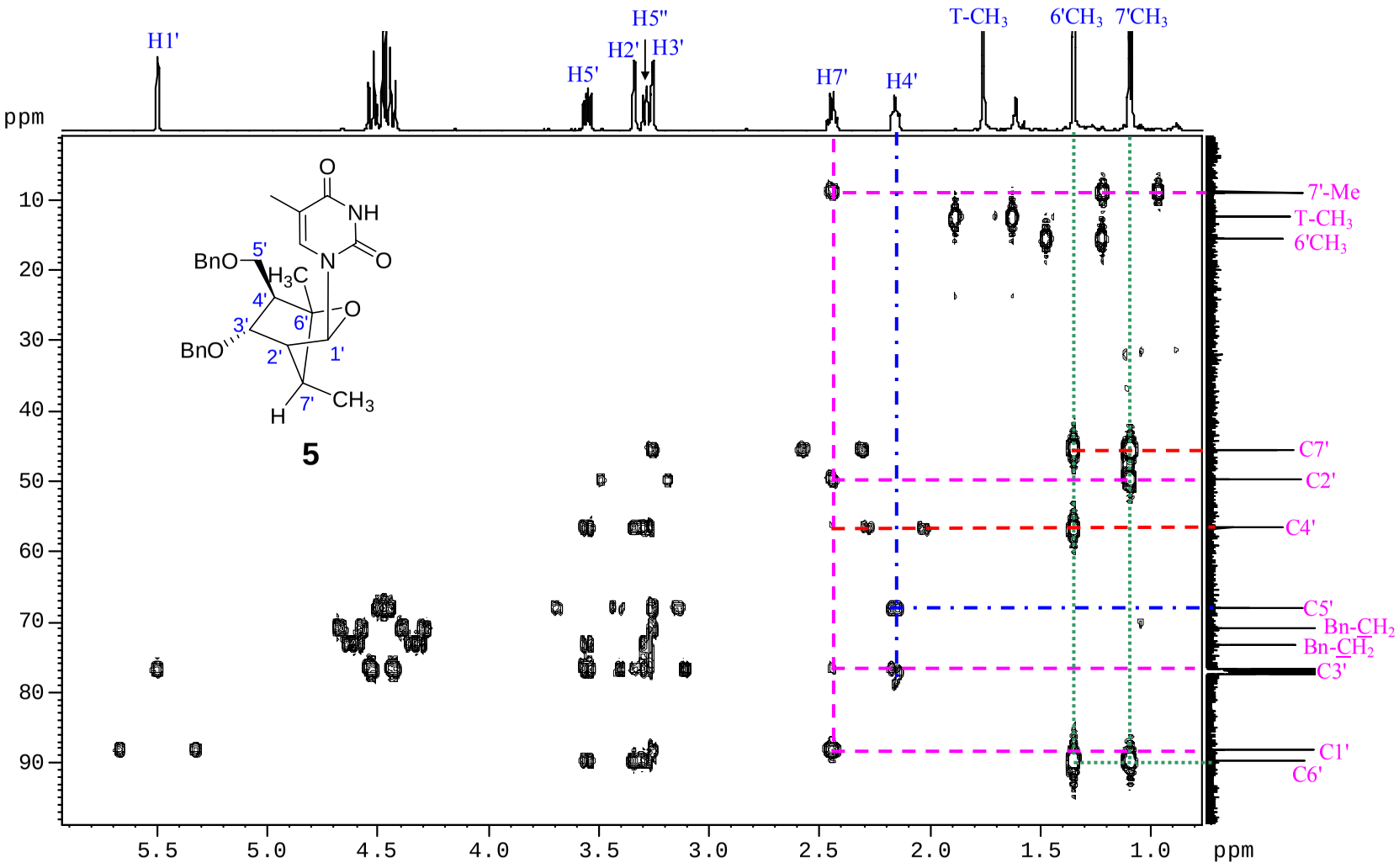


**Figure S29. expension of HMBC spectrum of compound 5.**

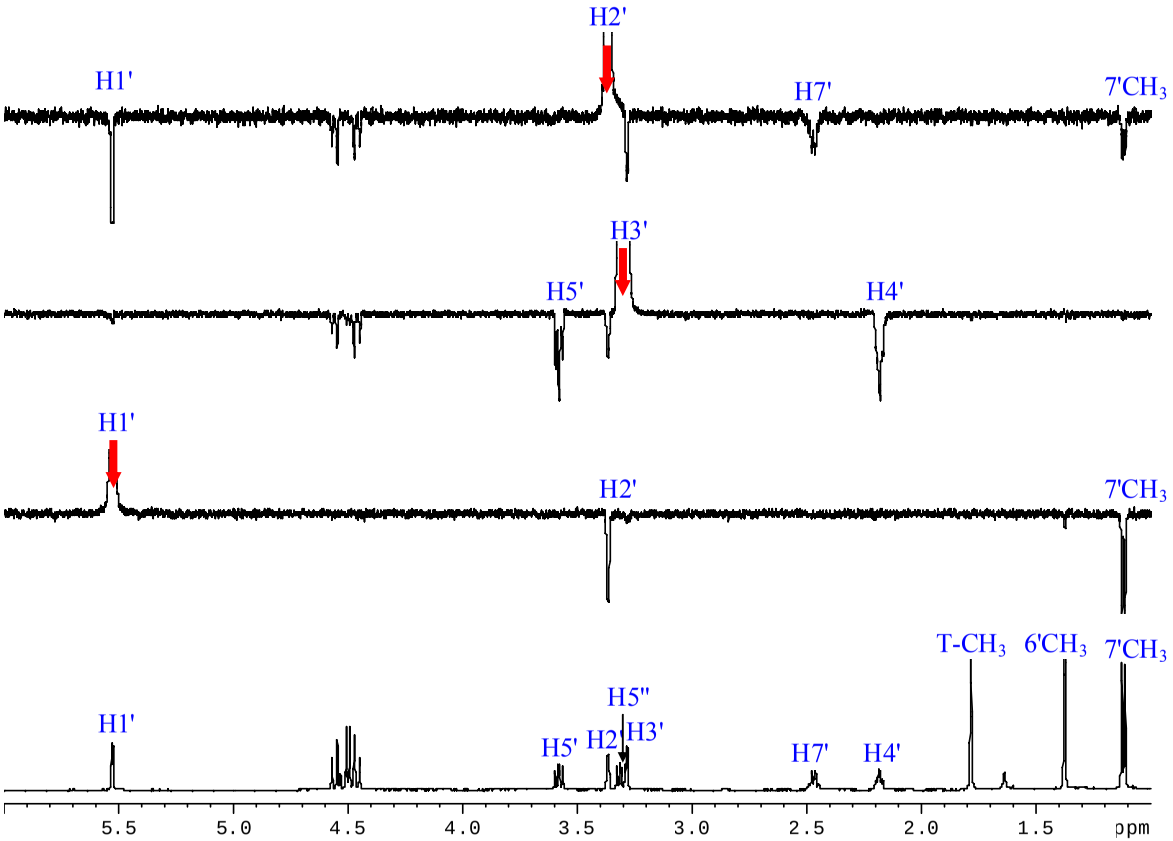


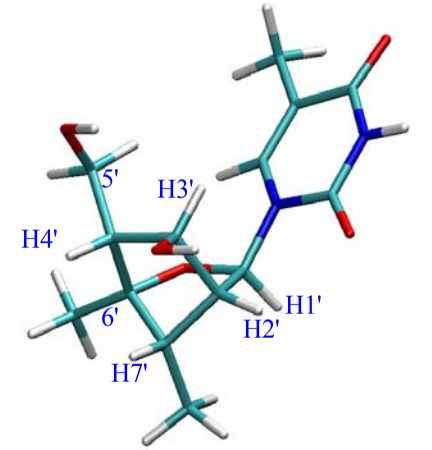


**Figure S30. 1D nOe spectra of compound 5.**

The model of product **5** shown on the right was obtained by ab initio geometry optimization.

**Figure S31. Homodecoupling spectra of compound 5.**

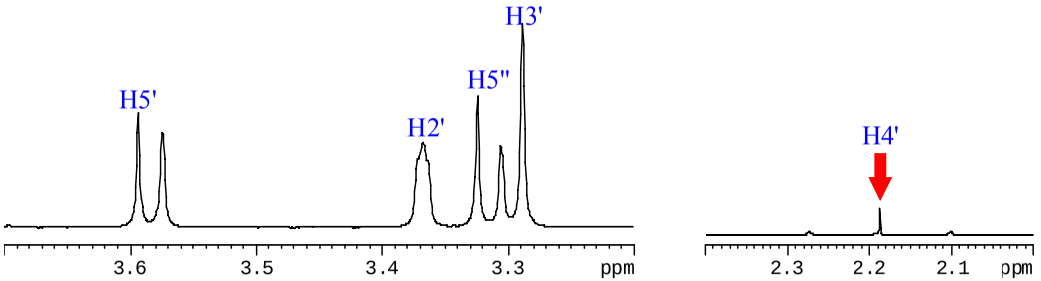


**(A)** Irradiation at H4' to simplify the H5', H5" and H3'.

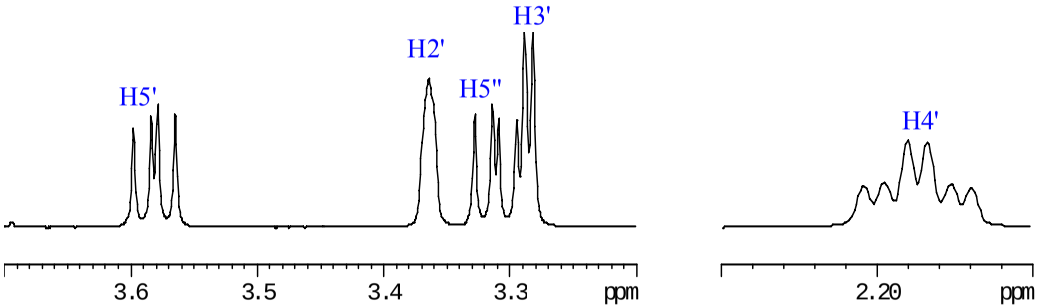


**(B)** $^{1}$H NMR of compound **5**.

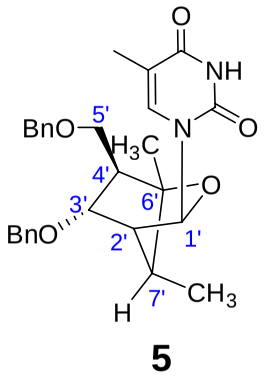


**5**

Compare (A) and (B), following coupling constants can be obtained: $J_{H4', H5'}$ = 6.9 Hz, $J_{H4', H5''}$ = 6.9 Hz, $J_{H4', H3'}$ = 3.2 Hz, $J_{H5', H5''}$ = 9.5 Hz.

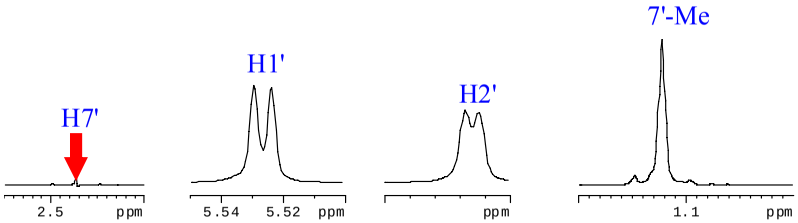


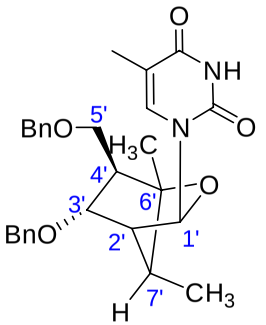


**5**

(**A**) Irradiation at H7' to simplify the H2', 7'-Me. $J_{H1', H2'}$ = 3.1 Hz, $J_{H2', H7'}$ = 1.5 Hz, $J_{H7', 7'CH3}$ = 6.9Hz

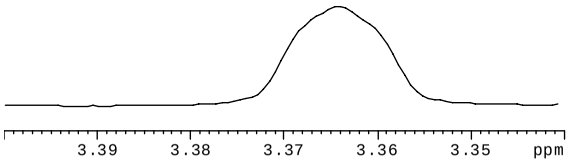


(**B**) Experimental $^{1}$H NMR spectrum of H2'

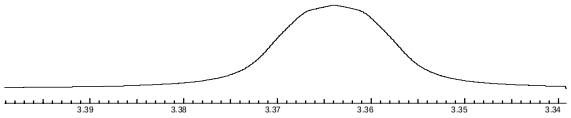


(C) Simulation of H2' with $J_{H1', H2'}$ = 3.1 Hz, $J_{H2', H7'}$ = 1.5, $J_{H2', H3'}$ = 1.3 Hz.

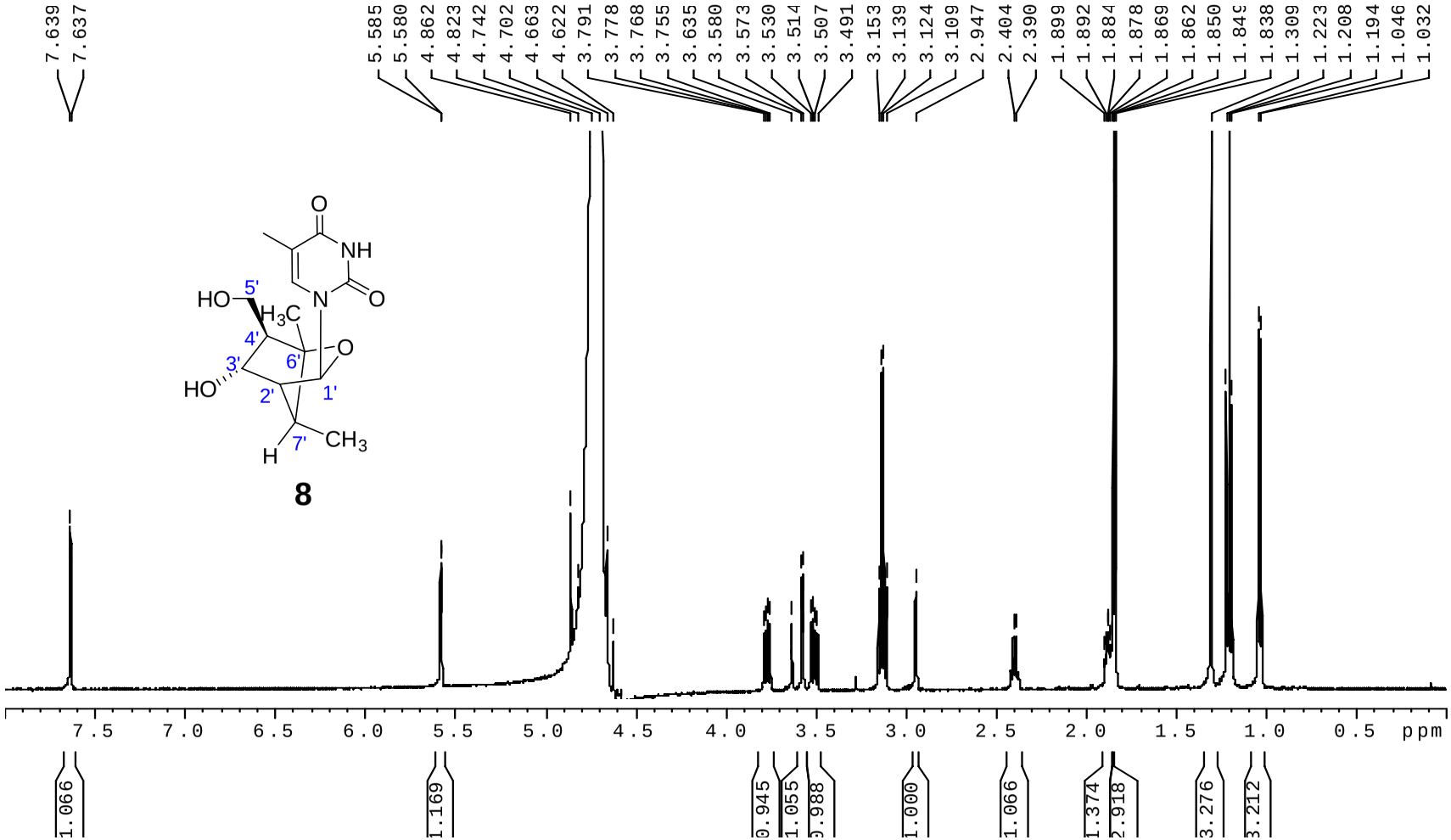


**Figure S32. $^{1}$H NMR spectrum of compound 8.**

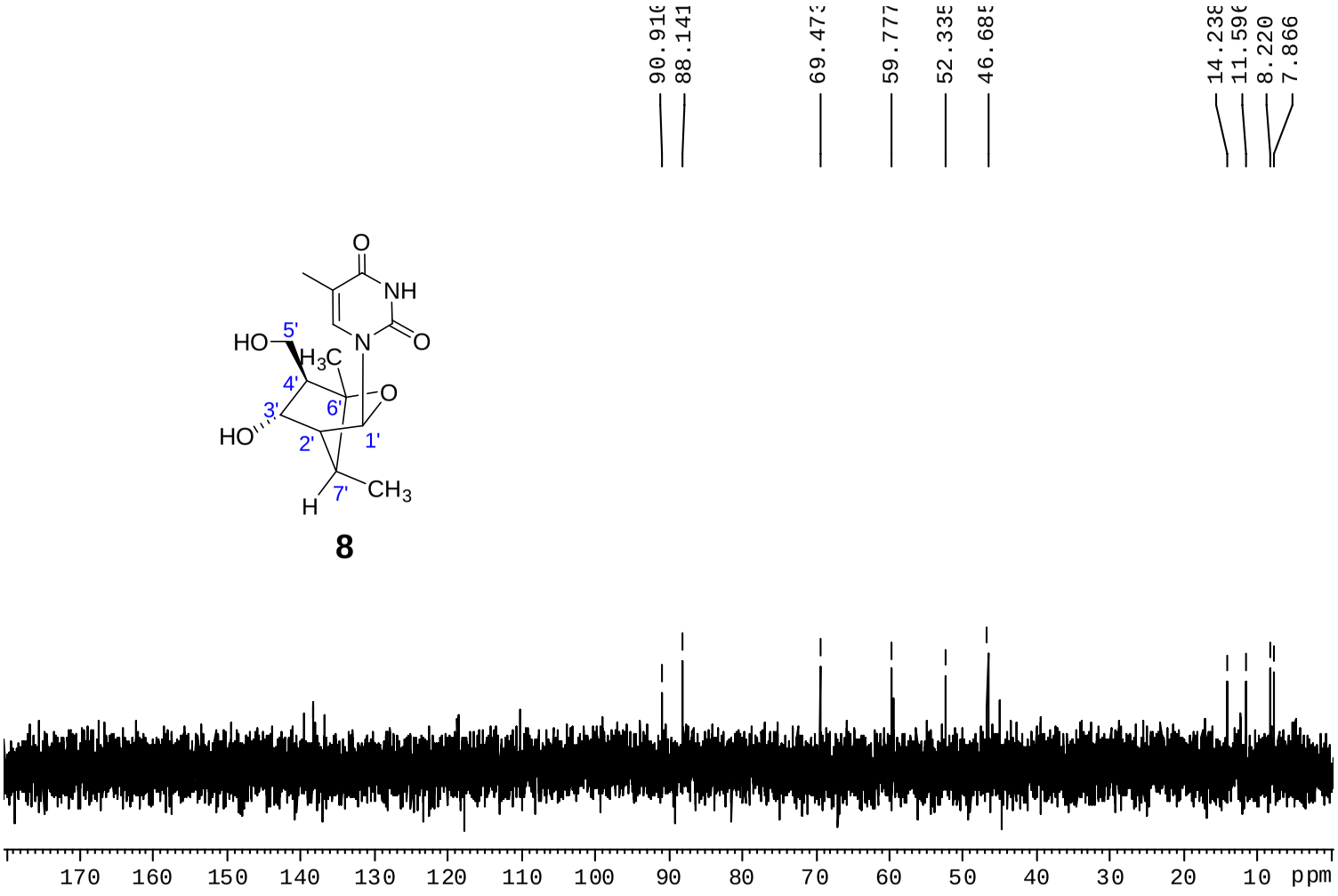


**Figure S33. $^{13}$C NMR spectrum of compound 8.**

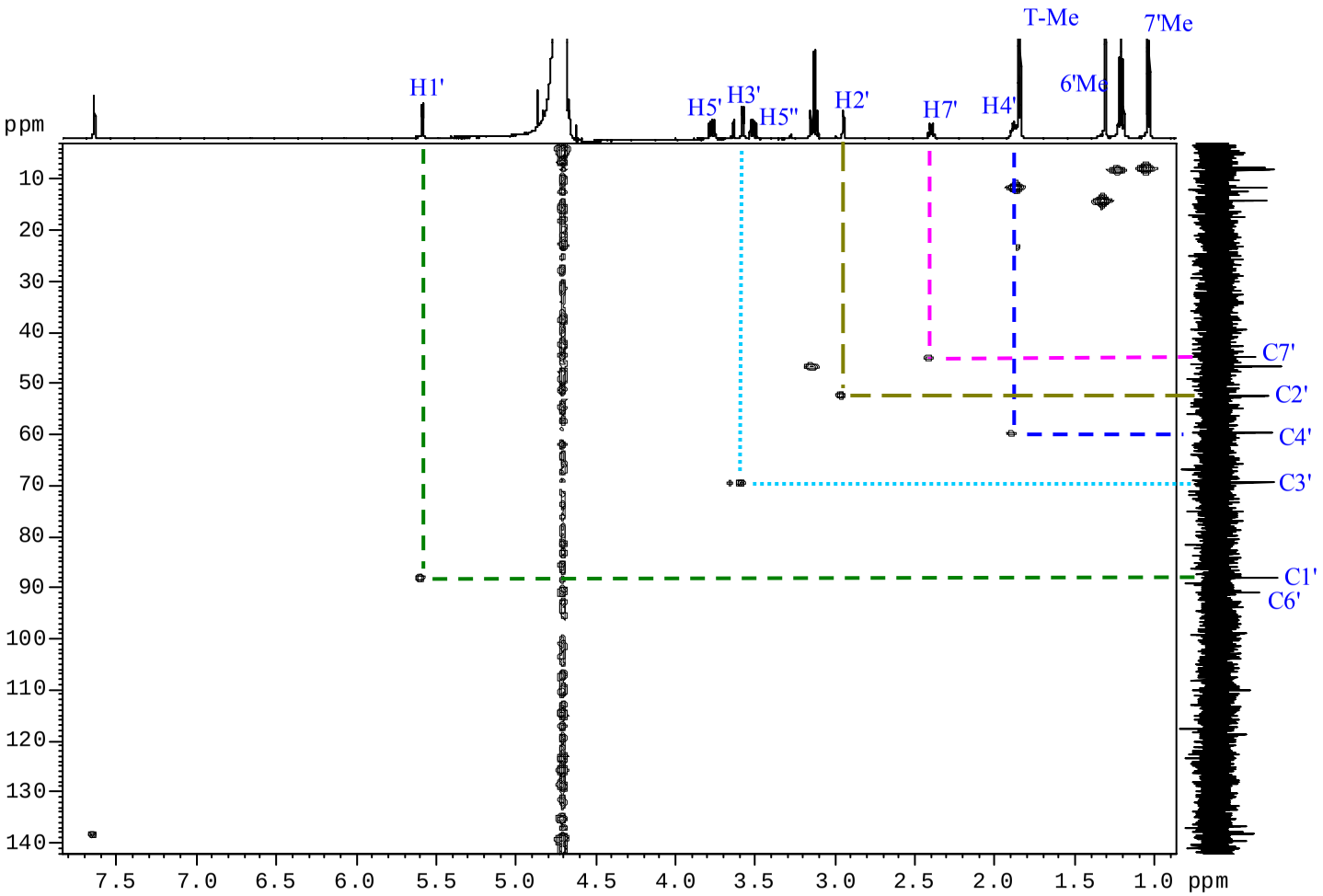


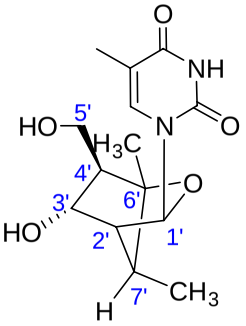


**8**

**Figure S34. HMQC spectrum of compound 8.**

**Figure S35. Homodecoupling spectra of compound 8.**

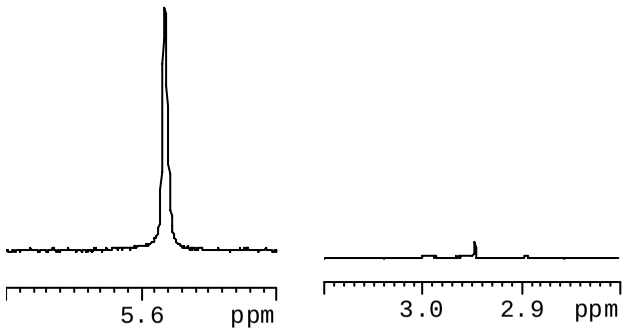


**(A)** Irradiation at H2' to simplify the H1'.

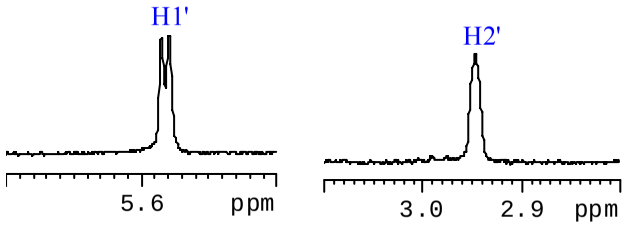


**(B)** $^{1}$H NMR of compound 8.

Comparation of (A) and (B) to get $^{3}J_{1',2'}$ = 2.8 Hz.

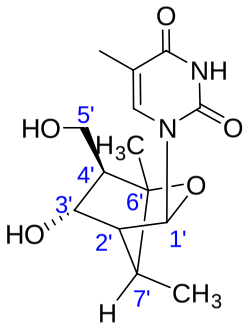


**8**

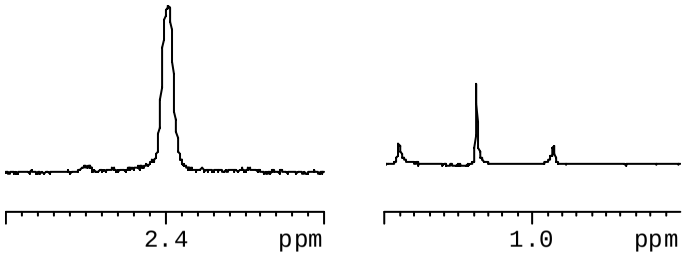


**(A)** Irradiation at 7'Me to simplify the H7'.

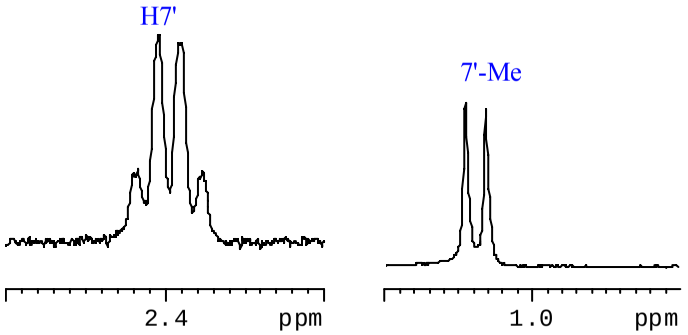


**(B)** $^{1}$H NMR of compound 8.

Comparation of (A) and (B) to get $^{3}J_{7',7'Me}$= 6.9 Hz, $^{3}J_{2',7'}$= 1.6 Hz

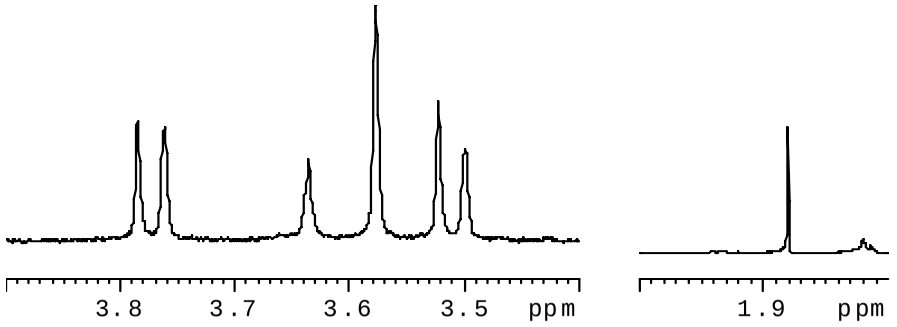


**(A)** Irradiation at 6'Me to simplify the H6'.

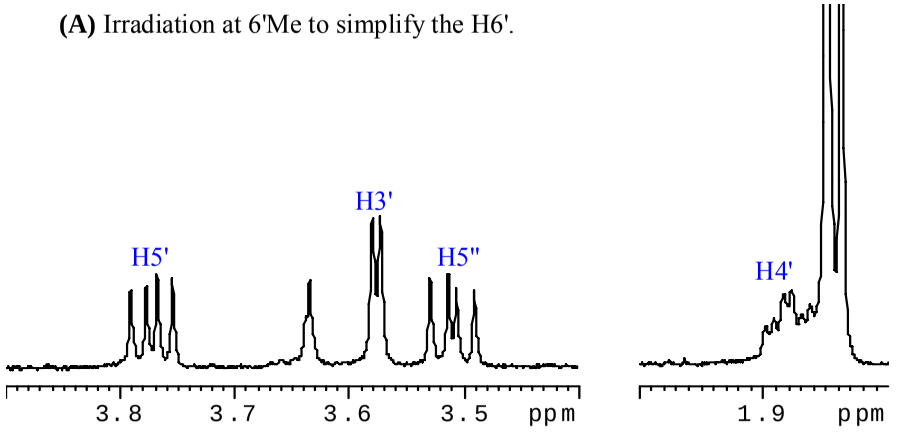


**(B)** $^{1}$H NMR of compound 8.

Comparation of (A) and (B) to get $^{3}J_{3',4'}$= 3.4 Hz, $^{3}J_{4',5'}$= 6.8 Hz, $^{3}J_{4',5''}$= 7.9 Hz.

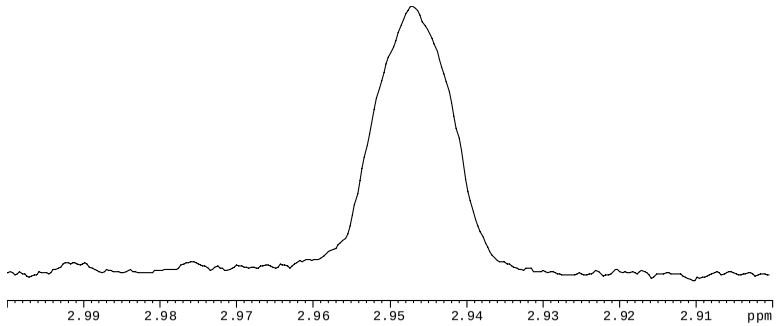


**(A)** Experimental spectra of H2'.

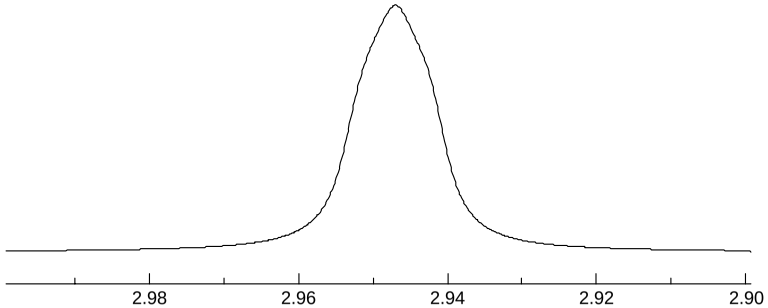


**(B)** Simulation of H2' spectrum with $^{3}J_{1',2'}$= 2.8 Hz, $^{3}J_{2',3'}$= 0.8 Hz, $^{3}J_{2',7''}$ 1.6 Hz

**Table S1. Total ground state energies (a.u.) and relative energies[a] (kcal/mol) of possible radical intermediates and products of the radical reaction of 5-membered carbocyclic-LNA-type and 6-membered carbocyclic-ENA-type thymidine nucleosides (Scheme 1).[b]**

| Intermediates & Products | Molecular structure | Total energy (a.u.) | Relative energy (kcal/mol) | Intermediates & Products | Molecular structure | Total energy (a.u.) | Relative energy (kcal/mol) |
|---|---|---|---|---|---|---|---|
| | | | | | | | |
| **4a** | 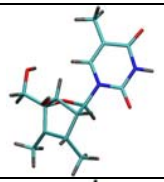 | -1030.8052742 | 0.0 | **9a** | 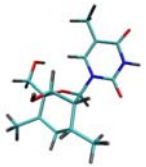 | -1070.139565 | 0.0 |
| Transition state from **4a** to **4b** | 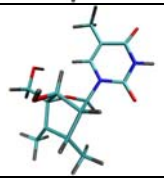 | -1030.8049393 | 0.21 | Transition state from **9a** to **9b** | 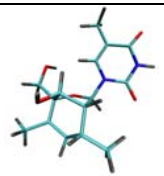 | -1070.1352318 | 2.72 |
| **4b** | 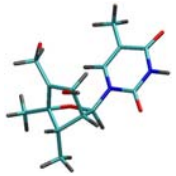 | -1030.8076751 | -1.51 | **9b** | 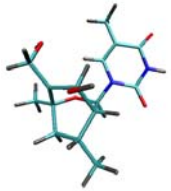 | -1070.1375917 | 1.23 |
| **Product (6)** | 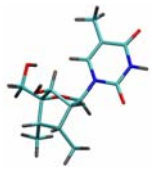 | -1031.4660989 | -99.57 | **Product (10)** | 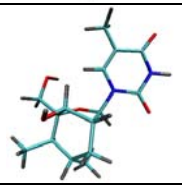 | -1070.7926769 | -94.73 |

| | | | | | | | |
|---|---|---|---|---|---|---|---|
| **Product (7)** | 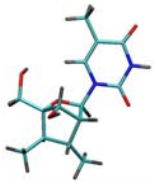 | -1031.4677692 | -100.61 | **Product (11)** | 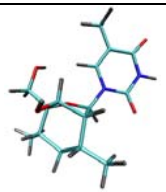 | -1070.8024227 | -100.84 |
| **Product (5)** | 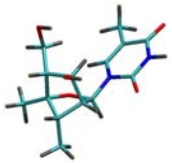 | -1031.4670787 | -98.67 | **Possible Product(II)** | 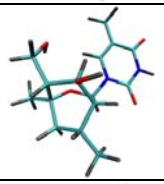 | -1070.7998757 | -99.24 |
| **Possible Product(I)** | 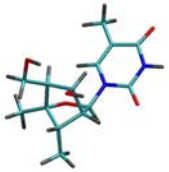 | -1031.4712652 | -101.30 | **Possible Product(III)** | 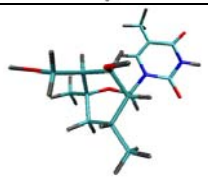 | -1070.7960901 | -96.87 |

[a] calculated relative to the 4a ground state energy for products (6) and (7) and relative to the 4b ground state energy for the possible products I as well as product (5)

[b] The geometry optimizations of the modified nucleosides have been carried out by GAUSSIAN98 program package[1] at the Hartree-Fock level using 6-31G** basis set and the total energies have been obtained employing Becke 3-Parameter (Exchange), Lee, Yang and Parr (B3LYP) correlation density functional theory (DFT) and bigger 6-311+G(d,p) basis set.

**Table S2. Some parameters of the *ab initio* optimized molecular structures of the radical intermediated 4a and 9a (Scheme 1).**

| Compound | *d*(*O*4'-*C*4')/Å | *d*(*O*4'-*C*6')/Å | *O*4'-*C*4'-*C*6' | *O*4'-*C*4'-*C*6'-C6'Me | *Angle between* $P_{C6'}$ and $\sigma^*_{O\,4'\text{-}C\,4'}$ |
|---|---|---|---|---|---|
| 4a | 1.444 | 2.379 | 107.14° | -80.82° | 5° |
| 9a | 1.433 | 2.409 | 109.45° | -154.48° | 51° |

**Table S3. Comparing the pentose sugar conformation of radical 4a and 9a.**

| | $\nu_0$ | $\nu_1$ | $\nu_2$ | $\nu_3$ | $\nu_4$ | *P* | $\nu_{max}$ | $\chi$ |
|---|---|---|---|---|---|---|---|---|
| 4a | -0.69 | -34.82 | 53.33 | -54.94 | 36.35 | 19.20 | 56.47 | -161.81 |
| 9a | -1.32 | -27.32 | 43.45 | -44.83 | 29.56 | 19.89 | 46.20 | -149.23 |

Reference:


[1] M. J. Frisch, G. W. Trucks, H. B. Schlegel, G. E. Scuseria, M. A. Robb, J. R. Cheeseman, V. G. Zakrzewski, J. Montgomery, J. A., R. E. Stratmann, J. C. Burant, S. Dapprich, J. M. Millam, A. D. Daniels, K. N. Kudin, M. C. Strain, O. Farkas, J. Tomasi, V. Barone, M. Cossi, R. Cammi, B. Mennucci, C. Pomelli, C. Adamo, S. Clifford, J. Ochterski, G. Petersson, P. Y. Ayala, Q. Cui, K. Morokuma, D. K. Malick, A. D. Rabuck, K. Raghavachari, J. B. Foresman, J. Cioslowski, J. V. Ortiz, A. G. Baboul, B. B. Stefanov, G. Liu, A. Liashenko, P. Piskorz, I. Komaromi, R. Gomperts, R. L. Martin, D. J. Fox, T. Keith, M. A. Al-Laham, C. Y. Peng, A. Nanayakkara, C. Gonzalez, M. Challacombe, P. M. W. Gill, B. G. Johnson, W. Chen, M. W. Wong, J. L. Andres, M. Head-Gordon, R. E. S., J. A. Pople, *Gaussian 98 (Revision A.6)*, Gaussian, Inc, Pittsburgh PA, **1998**.